GeoArabia, 2012, v. 17, no. 2, p. 81-116
Gulf PetroLink, Bahrain

Structural evolution of the northwestern Zagros, Kurdistan Region, Iraq: Implications on oil migration

László Csontos, Ágoston Sasvári, Tamás Pocsai,
László Kósa, Azad T. Salae and Athar Ali

ABSTRACT

The studied area in Kurdistan Region of Iraq lies across an important topographic/structural boundary between the southern lowlands and the northern, folded and imbricated Zagros Mountains. It also encompasses a prominent change in structural orientation of the northern Zagros, from a general NW-SE "Zagros" to an E-W "Taurus" trend. Geological mapping and structural observations, both in the mountains (Mesozoic–Palaeogene) and in the lowlands (Neogene), led to the following conclusions. (1) The oldest recorded deformation is a layer-parallel shortening, coupled with southwest-vergent shear that was followed by major folding of ca. 10 km wavelength and ca. 1,000 m amplitude. Even the Upper Miocene–Pliocene Bakhtiari Formation has steep to overturned beds in some parts, and synclines preserve syn-tectonic strata of Neogene–Pliocene age. Box folding is associated with crestal collapse, internal thrusting in the core and with formation of systematic joint sets. (2) On the southern limb of the major folds, thrusting of variable offset can be observed. The thrusts on the southern and northern limbs are considered responsible for the major uplift during main folding. (3) *En-échelon* fold-relay patterns suggest left-lateral shear along the EW-oriented segment and right-lateral shear along the NW-oriented segment. (4) A quick-look qualitative analysis of striated fault planes suggests a variable shortening trend from NE-SW to N-S, and some rare NW-SE shortening all associated with thrust faults. (5) The general structural setting of the area is linked to the north-eastwards to northwards propagation of the Arabian Margin beneath Eurasia. The ca. 30° bend in the mountain chain may be explained by the original shape of the Arabian Margin, or by pre-existing tectonic zones of E-W orientation in the northern part. Several observations suggest that there was no oroclinal bending (i.e. major rotation) of different parts of the chain, but the structures simply molded on their local buttress (almost) according to present orientations. However, a limited amount of rigid-body rotation in the different segments cannot be ruled out. The changing shortening directions generated several structural combinations on both the NW-SE Zagros and the E-W Taurus segments of the arc, many of which are still preserved. (6) Spectacular bitumen seepage in Upper Cretaceous and Palaeocene limestone originates from fractures or geodes of these formations. Many of these bitumen-filled voids are linked to the above-described Late Neogene–Recent shortening-folding process; therefore hydrocarbon migration into these voids is interpreted to be very young. This contradicts earlier ideas about massive Late Cretaceous breaching and bleeding off of hydrocarbons in this region.

INTRODUCTION

The studied area is located around the city of Aqra about 100 km north of Erbil, the capital of Kurdistan Region of Iraq (Figure 1). The area was the subject of a structural analysis and mapping work including the analysis of satellite photos and visits to selected outcrops. The study area is important for two reasons:

1. It contains a sharp topographic boundary between the southern lowlands and abruptly rising northern mountains, possibly corresponding to the Mesopotamian Foredeep and the Simply Folded zones of the Zagros Mountains (e.g. Bretis et al., 2011; Chalabi et al., 2010);
2. It is located where the strike of the chain changes from NW-SE *Zagros Trend* to E-W *Taurus Trend* (Figure 1).

The study area also comprises the Bekhme (Peris) Gorge and Zonta Gorge (Figure 1), which contain key exposures in Iraq as well as bitumen shows in Cretaceous and Palaeocene carbonates. The main aims of the paper are to: (1) give a more detailed description of the observed structural forms, (2) describe a possible structural evolution of the regions, and (3) link these aspects with observations on hydrocarbon migration.

GENERAL GEOLOGY

Main Structural Trends

The study area comprises the first mountain range between the Mesopotamian Foredeep and the Zagros Mountains, in which a marked change in structural style occurs from north to south (Figure 1a, b). A prominent feature of the area is a bend of ca. 30° in the structural trend between the northwest strike of the Zagros Mountains to the south and an E-W strike of the Taurus Mountains towards the Bitlis Suture of southern Turkey and the Sinjar Mountains of Iraq and northern Syria. This change in trend occurs in the heart of the study area, practically within the Bekhme Anticline. The broader neighbourhood of the study area can be divided into three belts from north to south.

The first belt lies to the north and is characterised by the highest mountains (Figure 1a). Near the Turkish-Iranian border the main structural unit is the ophiolite nappe and related deep-sea sediments emplaced along the High Zagros Thrust (Figure 1a). Thrust emplacement was initiated in the Turonian and ended in the Late Neogene, since the front of the nappe lies upon Neogene sediments (Spaargaren, 1987; Sissakian, 1997). The other main structural lineament, the right-lateral Main Recent Thrust (e.g. Blanc et al., 2003; Navabpour et al., 2007), does not appear to continue in Iraqi Kurdistan; or at least its sharp topographic expression in Iran fades away. This zone seems to splay into smaller faults towards Turkey, to be terminated in the Yüksekova Basin (Figure 1a).

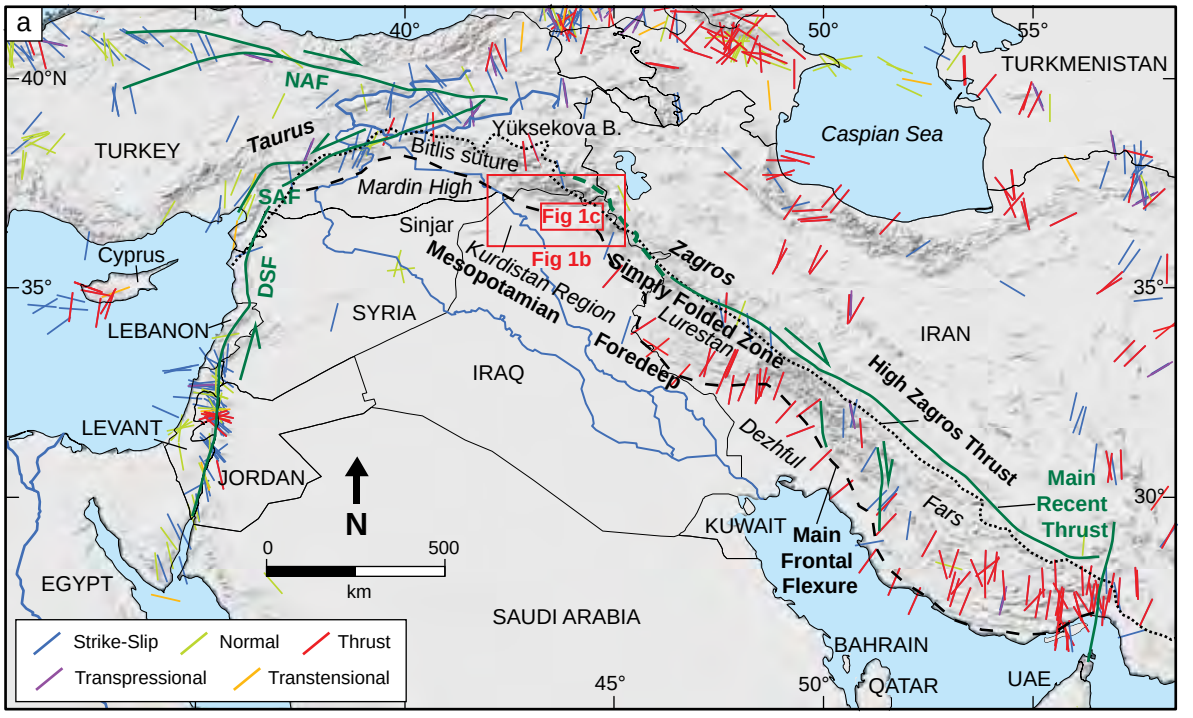

Figure 1: (a) Location of the study area projected on regional Digital Terrane Map with recent stress trends and stress environments (from Heidbach et al. (2008) available on-line at www.world-stress-map.org). Main geological elements after Kaymakci et al. (2010), Sissakian (1997) and Spaargaren (1987). NAF and SAF = North and South Anatolian Fault; DSF = Dead Sea Fault.

See facing page for continuation.

The second belt is named in Iran the "Simply Folded Zone" (e.g. Blanc et al., 2003; Homke et al., 2004). It is characterised by large regions of exposed Mesozoic rocks, deeply incised down to Triassic levels (Spaargaren, 1987; Sissakian, 1997). Most of the folds of this belt are thrust upon their southern neighbour. The Chia-i-Brandoz Anticline (Figure 1b) is thrust upon the Neogene Fars Formation, and therefore the age of final thrusting is Neogene. The southernmost elements of this second belt are the Bekhme and Aqra anticlines (Figures 1b and 1c) with a locally emergent thrust at their southern

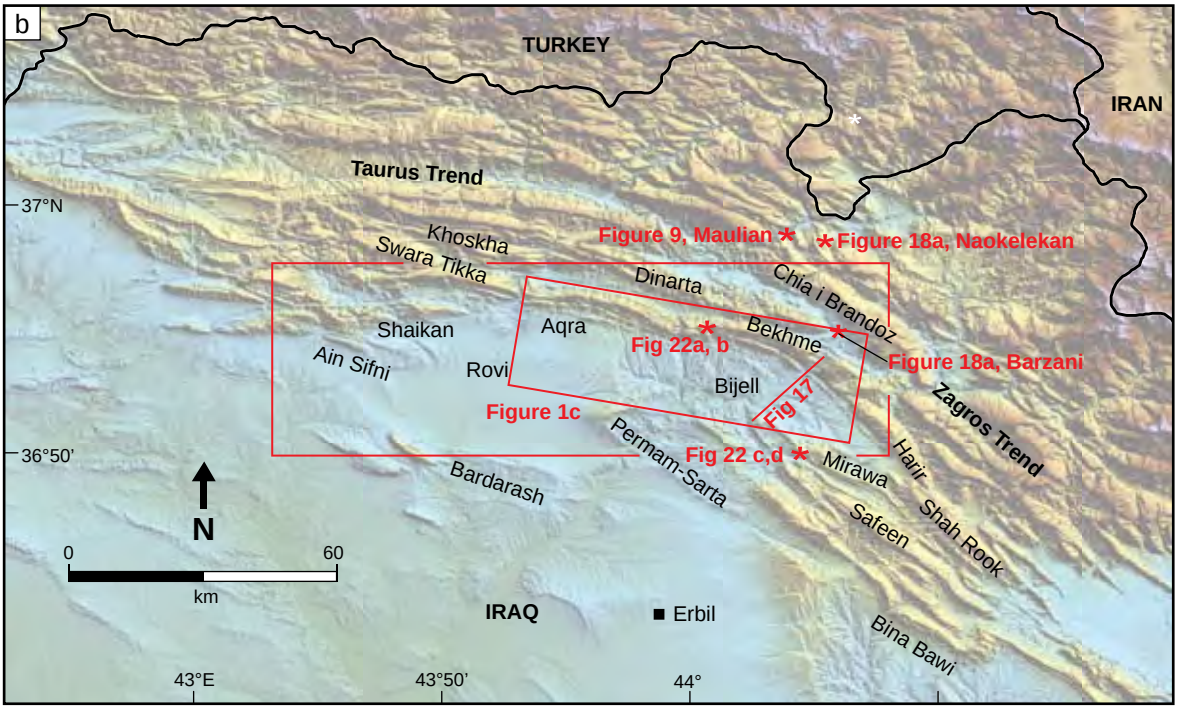

Figure 1: (b) Location map of Kurdistan Region of Iraq, based on 90 m digital terrane model (DTM) downloaded from NOAA. Study areas are marked by rectangles.

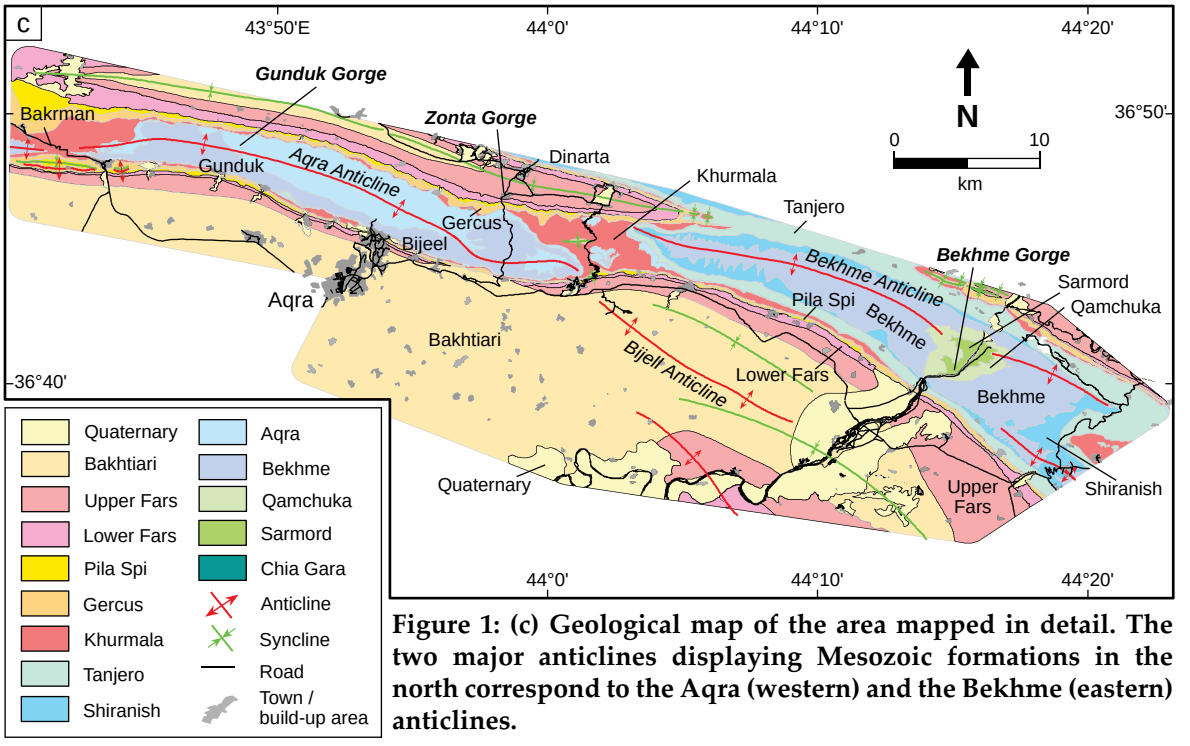

Figure 1: (c) Geological map of the area mapped in detail. The two major anticlines displaying Mesozoic formations in the north correspond to the Aqra (western) and the Bekhme (eastern) anticlines.

termination. The emergent anticlines near Bina Bawi (Figure 1b) also belong to the second belt. The main boundary corresponds to the topographic step between the "plains" and the "mountains" and is possibly a SW-vergent, deep and blind thrust. This hypothetic thrust fault is termed the Main Frontal Fault or Flexure (Figure 1a) in Iran (e.g. Blanc et al., 2003; Lacombe et al., 2006).

The third belt is located south of the "Simply Folded Zone", and is characterised by relatively flat topography with smaller anticlines. This belt, named the Mesopotamian Foredeep, has Eocene age rocks as the oldest exposed formations (Figure 1a, b, Figure 2). Based mainly on proprietary seismic examples, it seems that this zone is formed by more-or-less concentric folds, which are linked to inverted high-angle faults. Possibly there is a deep detachment, which may be located along evaporite strata of Early Jurassic, Late Triassic or Late Proterozoic age. The sharp topographic contrast between the Mesopotamian Foredeep and "Simply Folded Zone" does not seem to be reflected in the near-surface geology (see below).

General Stratigraphy of Kurdistan Region of Iraq

The stratigraphy of the area (see e.g. van Bellen et al., 1959/2005; Jassim and Goff, 2006; Figure 3) is characteristic for the whole of Iraq's Simply Folded Zagros. The sedimentary succession is possibly more than 10 km thick and quite probably begins with a ductile Upper Precambrian series. This is topped by a several thousand metre thick Palaeozoic–Lower Mesozoic succession, of which the shallow-water carbonates of the Permian Chia Zairi and Triassic Kurrachine formations form thicker, more rigid units. These are intercalated with thinner evaporitic and shaly beds that may be potential décollement horizons, near their base and top.

The Jurassic succession begins with a several hundred metres thick neritic carbonate, also generally rigid. In the Middle Jurassic this dolomitic platform passes laterally to evaporites (Alan and Adaiyah formations). In the upper Middle Jurassic and Upper Jurassic there is a widespread, yet thin basinal

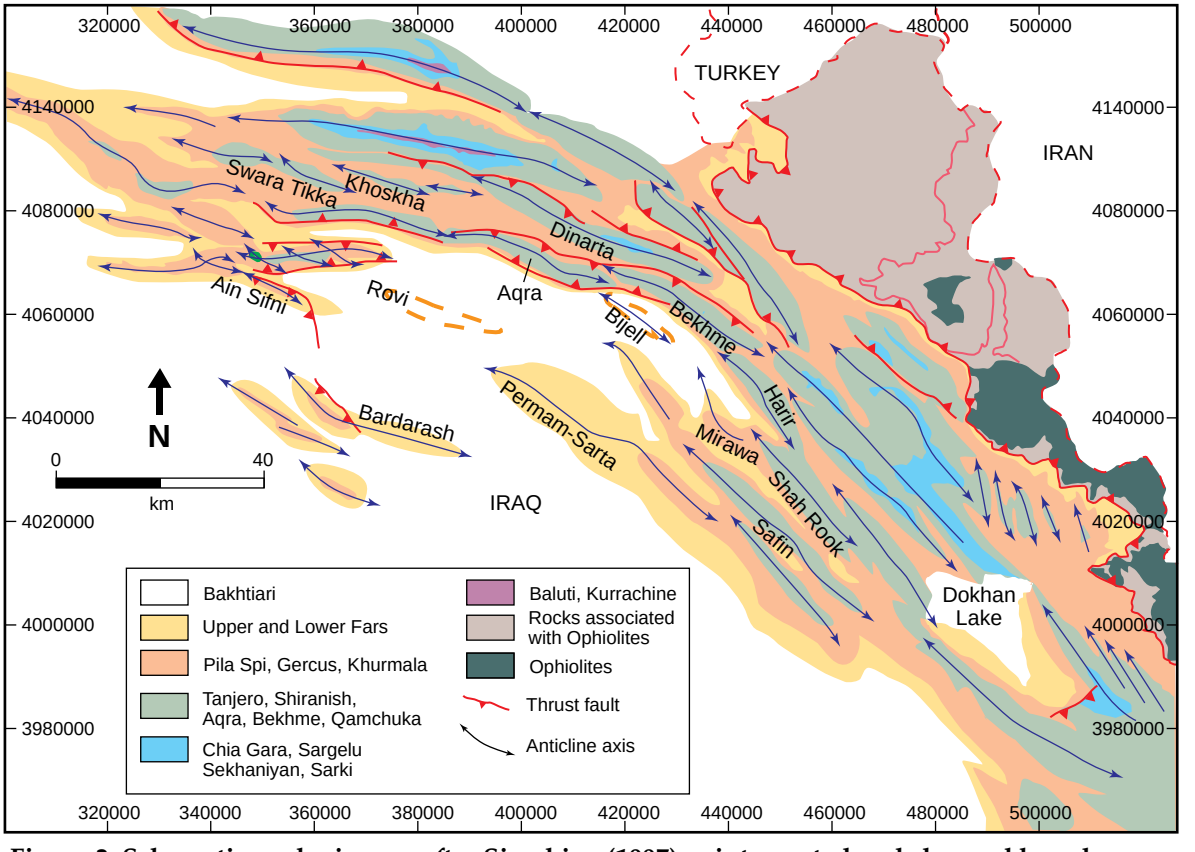

Figure 2: Schematic geologic map after Sissakian (1997), reinterpreted and changed based on our observations. The frame is identical to Figure 1b. Anticline axes and names marked on map.

facies, divided into the Sargelu and Naokelekan formations, which is believed to be one of the source rocks of the area. In regions exposed to compression these two formations might be effective décollements. In the Upper Jurassic the Sargelu and Naokelekan formations are overlain either by neritic dolomites (Barsarin Formation) or evaporites (Gotnia Formation) in this region.

In the Early Cretaceous the basinal sedimentary Chia Gara shale and marl was deposited. Locally this unit can also be a décollement. It passes upwards into the Sarmord/Balambo marl and then the Qamchuka neritic carbonate. Above a minor unconformity in the middle Cretaceous, an Upper

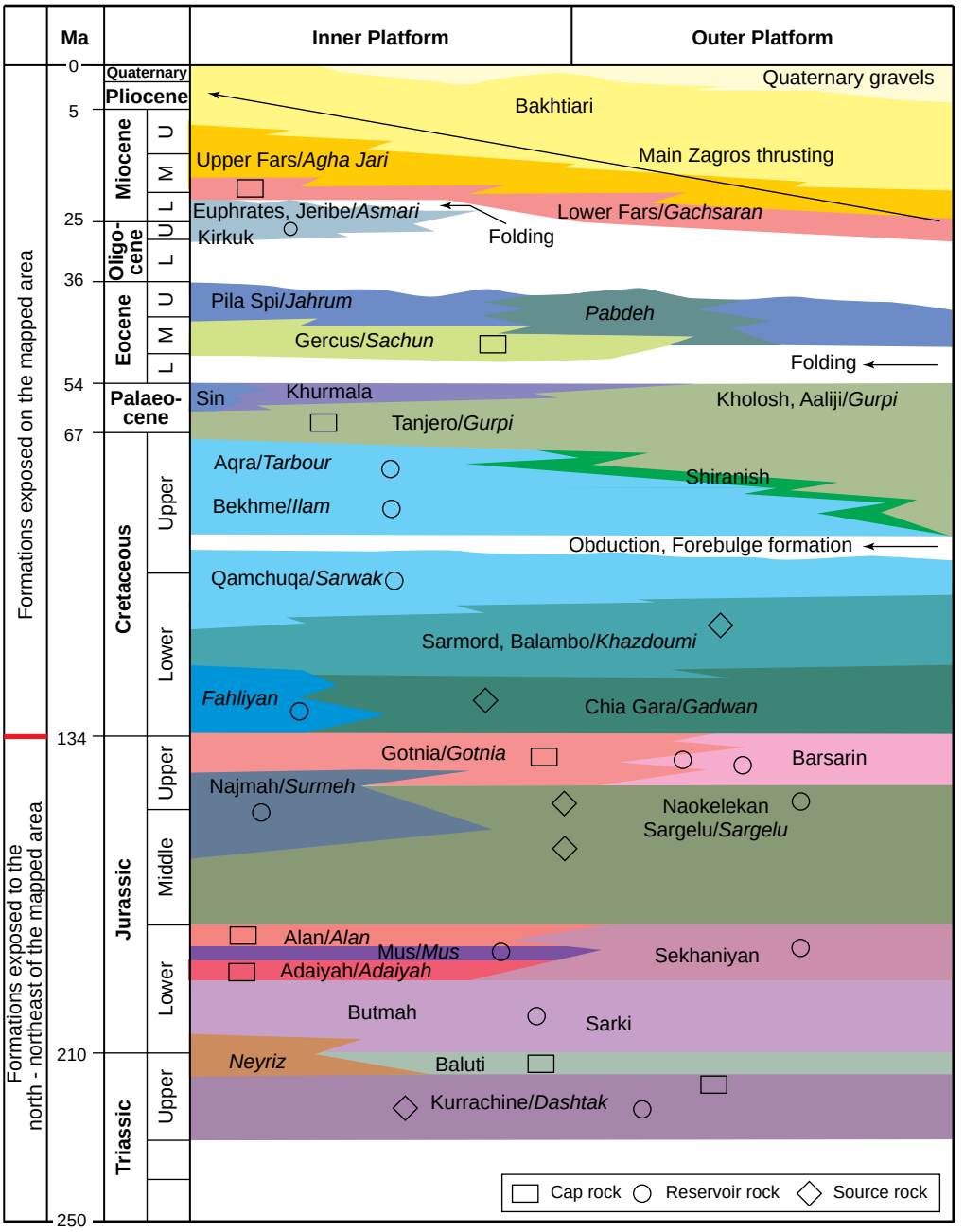

Figure 3: Stratigraphy of the study area. Note that the column is proportional to time, not to thickness. Formation names after van Bellen et al. (1959–2005). Sin = Sinjar. North Iraqi names marked by regular characters, their Iranian equivalents are marked by italics. The lowest exposed formation in the study area *sensu-stricto* is the Chia Gara Formation, but older formations are also exposed to the north. Tectonic events marked by black arrows. Source rocks, reservoirs, seals marked by diamonds, circles and box shape, respectively.

Cretaceous platform carbonate represented by the Bekhme and Aqra carbonate was deposited. This platform passes laterally and upwards into basinal sediments (Shiranish and Tanjero marl). The upper part of the deep-marine marl may also be Palaeocene in age (Kholosh Formation; Sarbazheri et al., 2009). The Cretaceous neritic carbonates (Qamchuka, Bekhme and Aqra formations) form a ca. 600 m thick rigid and weathering resistant structural level that can be used to determine the wavelength of folds. The Qamchuka and Bekhme formations form the core of most folds in the Kurdistan region (Figure 2).

A more rigid carbonate unit (Palaeogene Khurmala-Sinjar Formation) is overlain by very characteristic, brick-red Eocene clays forming a detachment horizon (Gercus Formation) and by a thin and chalky-dolomitic Eocene carbonate (Pila Spi Formation). This rigid unit forms very characteristic outcrop exposure patterns and is easily recognised even on satellite photos.

The Neogene is represented by (1) the sometimes evaporitic, variegated Middle Miocene Lower Fars Formation; (2) the mostly sandy, fluvial Middle–Upper Miocene Upper Fars Formation; and (3) the conglomeratic Upper Miocene–Pliocene Bakhtiari Formation (8 Ma and younger). All these formations are rarely and poorly dated (Jassim and Goff, 2006). Modern magneto-stratigraphic-isotope data (like Homke et al., 2004) are lacking. These Neogene formations have a cumulative thickness of more than 1,500 m.

OBSERVATIONS

Layer-parallel Shortening

Thrust Faults

Several sites indicate a layer-parallel shortening episode. The best examples can be seen in the Pila Spi Limestone, because multi-coloured clays form interlayers that separate the mechanically more brittle limestone beds. In the southern foothills of the Bekhme Gorge, and along the Bijeel-Dinarta road (Figure 1c), the Pila Spi Formation is folded with steep to subvertical layers (Figures 4a and 4b). The stiff limestone layers carry smaller internal thrusts, which detach in adjacent clay layers. When bedding was re-tilted to horizontal, thrusts formed a conjugate set and defined a SW-directed, layer-parallel shortening (Figures 4c and 4d).

Cleavage

In some cases, marly layers show traces of incipient cleavage, which is irregular and dense (Figure 5). The cleavage planes are parallel to each other and oblique to layering. Penetration depends on the competence of the affected material. Layering may be tilted, folded, but the characteristic angular relationship is preserved (Figures 5a and 5b). Geometrical relationships suggest that when bedding was re-tilted to horizontal a NE-SW layer-parallel shortening with a SW-oriented shear component occurred along the layers (red traces on the stereograms of Figure 5d and 5h). The suggested sequence of events is explained on Figure 5j. Layer-parallel shear may have also been generated by flexural folding, but observed angular relationships are not conformable with this interpretation (Figure 5i).

Comparing the cleavage in the Bekhme and Aqra anticlines (Figures 5c and 5d *versus* 5g and 5h) indicates a slight rotation of ca. 15–20° between the two regions and shear directions. The shear directions inferred from cleavage correspond to a direction perpendicular to the local fold axis (see below). A dense fracture network / fracture cleavage is perpendicular to bedding and is interpreted as a systematic joint set (see below).

Layer-parallel Cavities

The Bekhme Formation and at least three massive horizons within the Qamchuqa Formation are pervasively dolomitised and fractured. The fractures are oriented in well-organised networks, either perpendicular, or parallel to layering. The fractures are apparently conducting fluids, since they host lighter colour overgrown crystals in cavities. Almost as a rule, these cavities are finely coated with

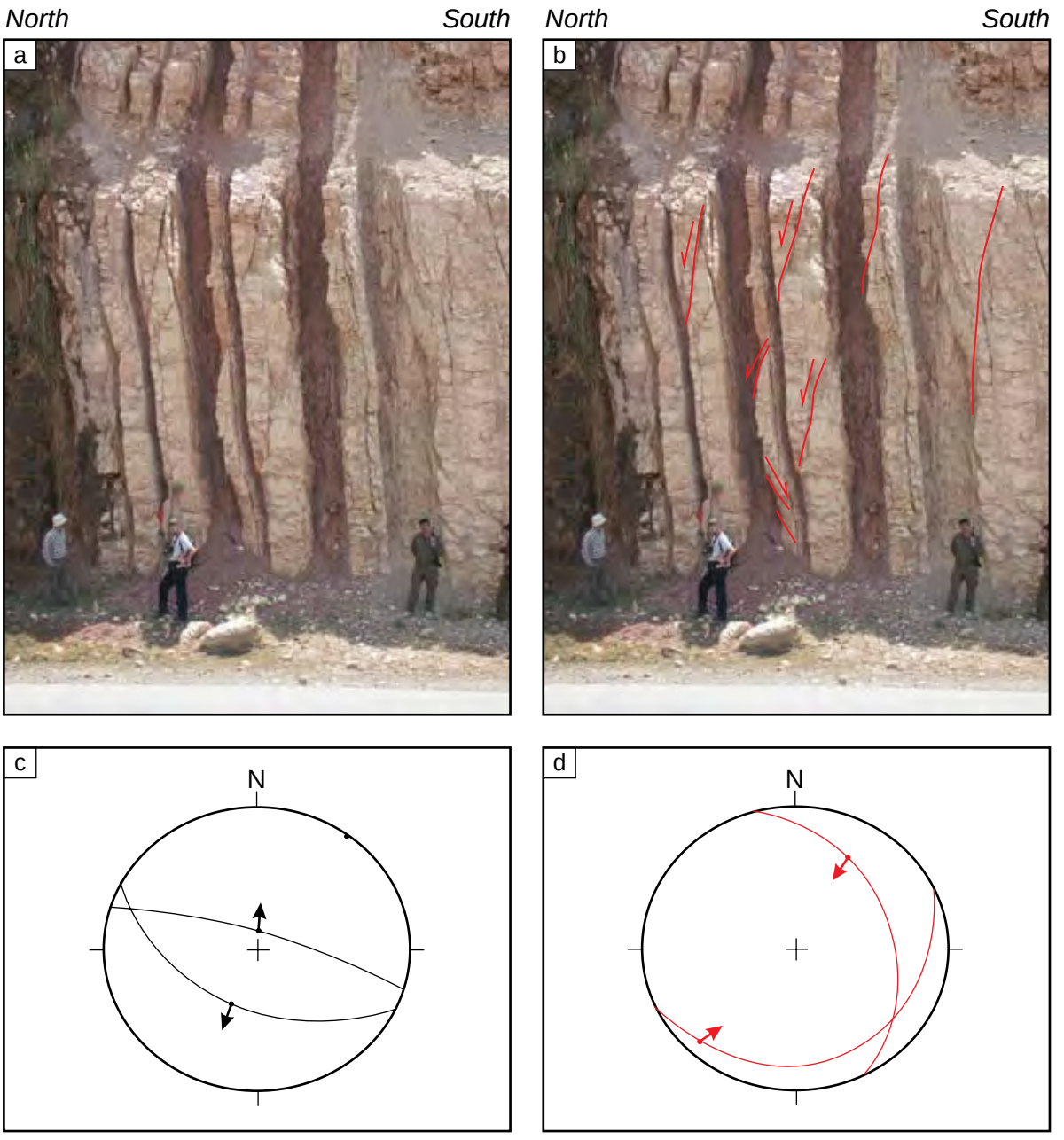

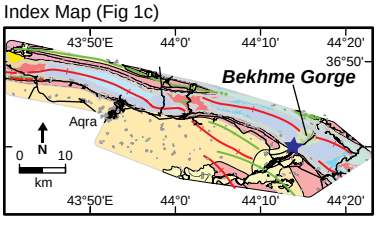

Figure 4: Pila Spi Limestone at the southern mouth of Bekhme Gorge, with subvertical dip. Small insert map with star shows the location of the exposure. (a) Uninterpreted field photo, and (b) with interpretation. Note the small thrusts (red) repeating individual layers and detaching in shaly interlayers. (c) Stereoplot (equal area projection; lower hemisphere) marks original measurements of bedding and shear surfaces. Dot = pole to bedding; Traces = measured thrust faults. Small arrows = slickenslide lineations with relative movement. Outward: normal; inward: thrust. (d) Stereoplot marks measurements of shear surfaces tilted back to bring bedding to horizontal. Red traces = back-tilted fault traces. Small arrows = same legend, as for (c).

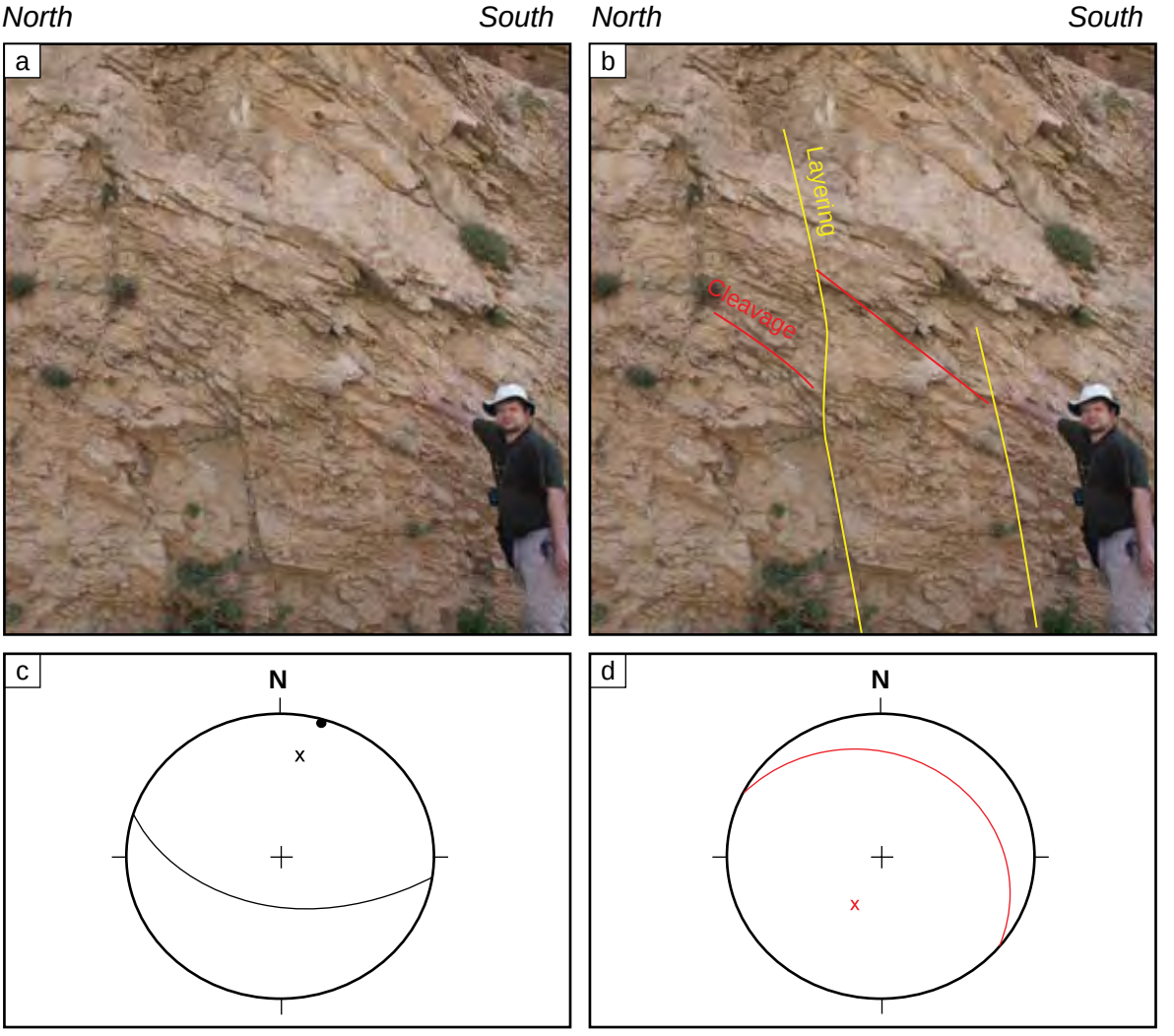

Figure 5: (a) Marlier facies of the Aqra Formation near the southern mouth of Zonta Gorge, uninterpreted. Small insert map with star shows the location of the exposure. (b) Same interpreted. Yellow marks layering, red marks incipient cleavage. Note the oblique pattern of cleavage with respect to bedding. Top-down shear direction along layers is deduced. (c) Stereoplots mark original measurements of bedding and cleavage. Same legend as for Figure 4. Crosses = pole to cleavage. (d) Cleavage dip back-rotated until bedding becomes horizontal.

See facing page for continuation.

euhedral crystals of calcite or dolomite. This means that crystals were precipitated from fluids after the fracturing process, in an open space, and were free to grow. The innermost part of these cavities is filled by bitumen (Figure 6).

While layer-perpendicular fracture sets are easily explained by joint formation induced by sedimentary / tectonic load or incipient folding, layer-parallel fractures need a more detailed explanation: it is very hard to open up fractures against normal stress induced by sedimentary load. The only plausible way to open such fractures is through layer-parallel shear. Indications for such shears were found in some well-developed, layer-parallel fracture zones (Figure 6). Most rhomb-shaped cavities opened up by layer-parallel shear were compatible with top-SW movement (Figures 6c and 6d, see explanation on Figure 6e), but some were compatible with top-NE shear (Figures 6a and 6b). The former fit into a general pre-folding layer-parallel shear event, while the latter can be explained by layer-parallel

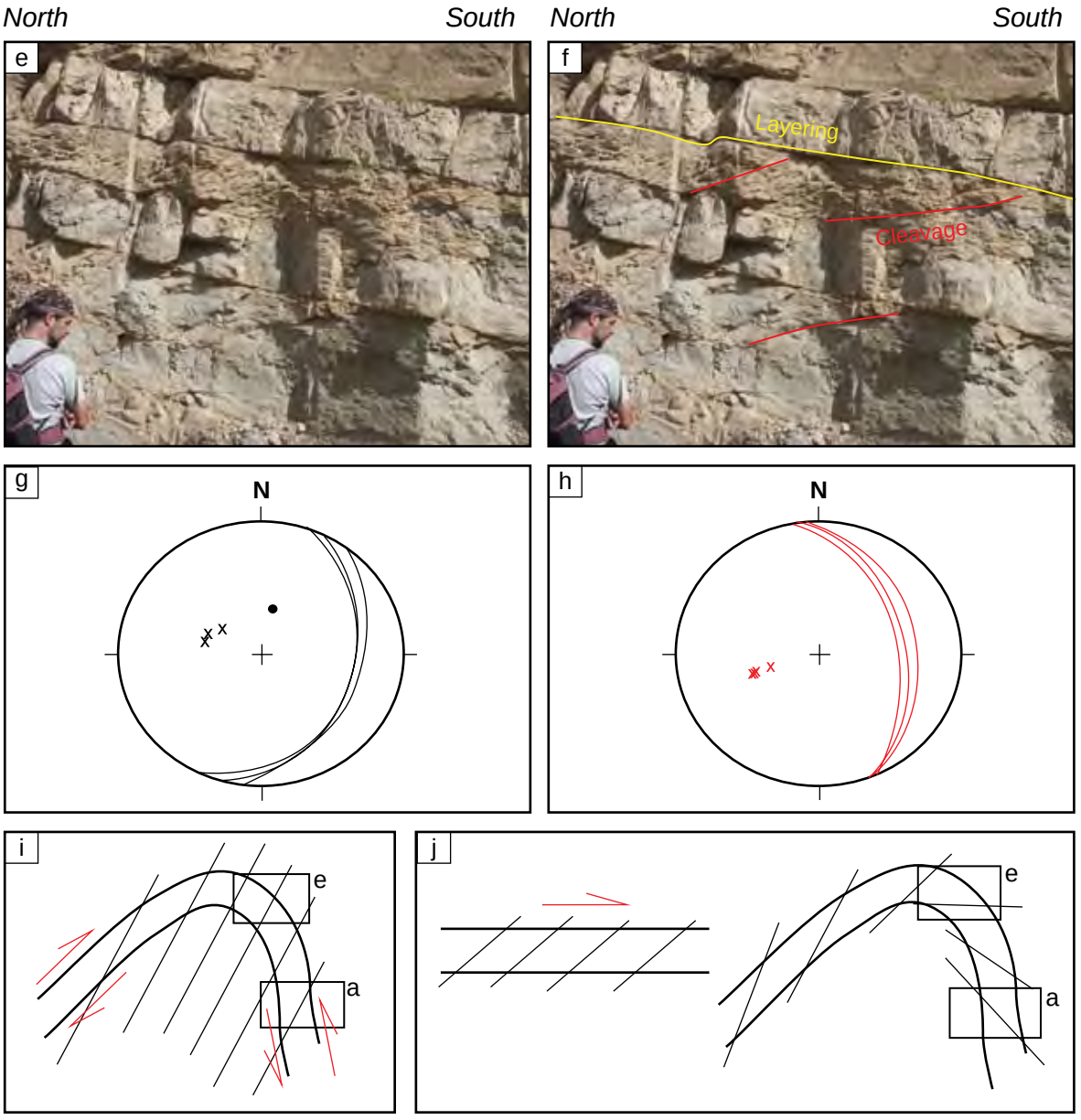

Figure 5: (continued). (e) Sarmord marl in the heart of Bekhme Gorge, uninterpreted. (f) Same, interpreted. Marlier beds carry penetrative incipient cleavage. Same colour code as in Figure (b). (g) Stereoplot marks original measurements of bedding and cleavage. (h) Same with reconstructed cleavage dip with bedding rotated to horizontal. Note top-southwest shear direction in both cases. Note also small divergence in orientation, that may correspond to different fold orientation. (i) Flexural fold model. Layering marked by thick, cleavage marked by thin lines. Cleavage is roughly parallel to axial surface. There is a shear (red arrows) on the limbs of the fold. (j) Model in which cleavage precedes folding. Same signs as for i. Left figure in original position, right figure in folded position. Small quadrangles mark the possible locations of photos of Figure 5.

slip due to flexural folding (see explanation Figure 5j). Although high fluid pressures may have contributed to fracturing, our fluid inclusion studies did not record any abnormal overpressure, but indicated deep burial of all Mesozoic formations; ca. 3,600 m for the Cretaceous formations.

Summary Layer-parallel Shear

When all above mentioned features are assessed, deformation can be interpreted as roughly homogenous if the layers are retro-folded until horizontal. In other words this shortening, coupled with mostly SW-oriented shear occurred in a pre-tilted and pre-folded state. Deformation should

be younger than Eocene (youngest observed features in Eocene) and hydrocarbon migration should have occurred synchronously or should have happened after the layer-parallel shear (voids and structures invaded by bitumen).

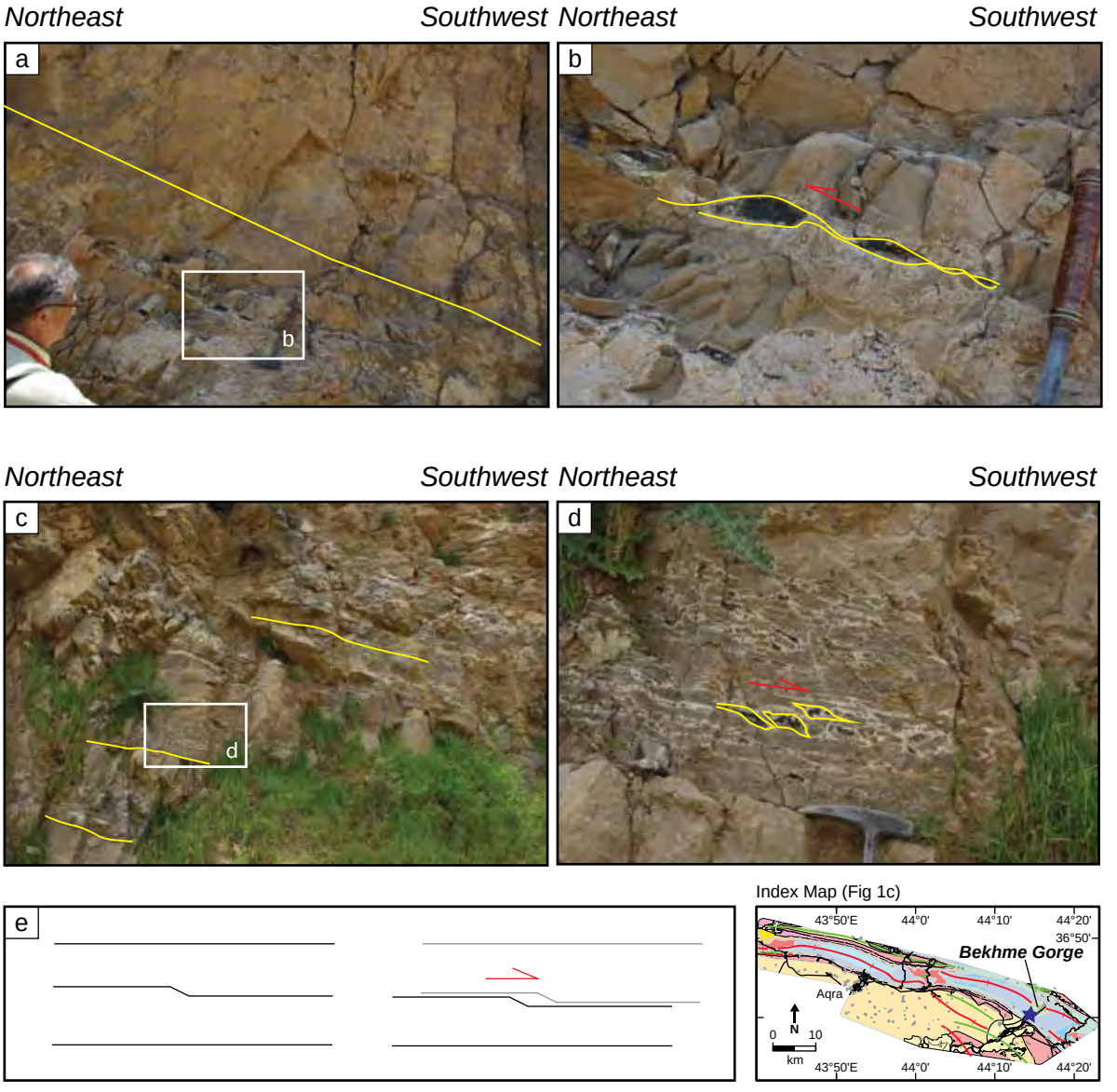

Figure 6: Layer-parallel cavities in Qamchuqa dolomite on the southern limb of the Bekhme anticline, in road cut. Note that all filled cavities make rhomb-shaped open gashes due to layer-parallel slip along non-separated parts of the fractures. (a) Overview photo of top-NE shear association. Yellow line marks layering. Insert box and (b), shows detail of such rhomb-shaped gashes. Red shear arrow indicates deduced shear direction. Yellow outlines mark the shape of rhomb-shaped cavity walls, that moved away due to shear. (c) Neighbouring exposure of Qamchuka dolomite on same southern limb, same location. Yellow lines mark layering. Insert box and (d), shows detail of rhomb-shaped gashes giving top-SW shear. Red shear arrow indicates deduced shear direction. Yellow outlines mark the shape of rhomb-shaped cavity walls. The cavities are coated with calcite-dolomite minerals and inner parts are filled by bitumen. (e) Model for formation of rhomb-shaped cavities. Original situation in left hand side, final situation in right hand side picture. Upper layer is pushed to the right, and small irregularity in slip surface results in a rhomb-shaped opening.

Major Folds

Folding of layers into major, roughly E-W- to NW-oriented folds is the most prominent deformation in the studied area. The topography closely resembles the folding in the study area (insert on Figure 1b). Only minimal erosion has occurred and all slopes are practically parallel to layering. The crestal areas are unaltered. A couple of gorges, up to 1,000 m deep, are incised into the antiforms perpendicular to their strike, near their periclinal terminations (Figures 1b and 2). Synclines are represented by regional valleys with young clay-rich sediments. The anticlines to the north of the study area are more deeply eroded and their cores better exposed.

Geomorphologic Character of Folds

The folds in our study area have lengths of 25–32 km and widths of 4–5.5 km, corresponding to a length-to-width aspect ratio of 4.5–7.5. These ratios plot in the transitional zone between detachment folds and ramp-related folds in the geomorphologic analysis of folds in Iran (Burberry et al., 2010, their figure 9). The symmetry of the folds is complex; their axial trace is curvilinear, and the folds change facing at different segments of the fold. In the following discussion it will be shown that the folds are linked with thrusts, frequently on both limbs.

Box Folds

Most of the folds are box-folds, with steep, relatively planar limbs that dip at 40–70° (Figures 7a and 7b). The limbs pass into sharp, poorly rounded hinges. The anticlinal shape in the Mesozoic succession is fairly simple. However, anticlines formed by the Khurmala or the Pila Spi Limestone are somewhat diverging from that simple shape (Figures 7c and 7d). The reason is that sometimes the Tanjero marl and more frequently the Gercus clay behave in a ductile manner, thus eventually causing the complete detachment of the fold geometries below and above. From Bijeel towards Aqra and Bakrman (Figure 1c) it is quite common to find steep southerly dips in the Mesozoic section on the southern limb of the anticline, while extra folds or steeply overturned (northerly) dips, are found in the Pila Spi, Fars, or even Bakhtiari formations (Figures 7c and 7d). Accordingly, the internal deformation of the Gercus clay can be very chaotic, and can range from tight to open folding, internal thrusting, to ductile thickness changes. Theoretically the divergence of geometric forms in the Palaeogene strata from the stiff Mesozoic core can be the result of gravity collapse of sediments gliding down on a ductile (Gercus) detachment. However, overturned beds are possibly not the result of such a gravity-driven process, because in some examples (e.g. southern mouth of Zonta Gorge) they are associated with thrust faults (see below). These divergent geometric forms are rather the expressions of thrust shear.

A box-fold shape creates space problems in both external and internal parts of the hinge zone. The axis-perpendicular, layer-parallel elongation in the external, and the similarly directed shortening in the internal part, should be accommodated by some structures. Extension in the outer arc (Figure 8i) was accommodated by large normal faults, creating crestal collapse (Figures 8a and 8b). The internal part of the folds is characterised by gentle disharmonic folding and a multitude of internal thrust surfaces (Figures 8c to 8f). These thrusts are repeating layers, or forming duplex structures. As a consequence, higher layers may have higher curvatures and steeper dips, whereas lower layers may have more gentle dips. The internal thrusts generally detach on more ductile layers within the same succession. The Sarmord and Balambo formations or Chia Gara shale preferentially form these detachment surfaces.

Dip Measurements

Dip measurements of bedding on stereoplots suggest that the folds are curved from a NW trend in the eastern part, towards an E-W trend in the western part of the area (Figure 9). When the measured or constructed fold axes are taken into account, there is a strong correlation between the local direction of the curvilinear axial trace and the measured local axes. However, even in the case of simple transects (like in the case of Gunduk Gorge or Bekhme Gorge), the measured bedding poles do not fit perfectly on a single girdle, i.e. the folds are not fully cylindrical. They rather show a distinct spread. Although the difference between these fold orientations is not large, it is still notable, and might suggest superposition of two different fold orientations.

Figure 7: (a and b) Aqra Anticline near Gunduk Gorge, with and without interpretation. Location marked on index map. Layering is marked by a yellow line. Note steep southern limb and small sharp hinge.

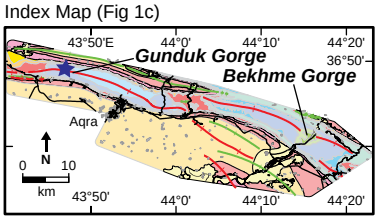

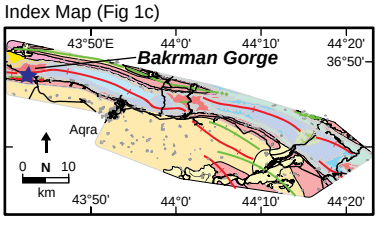

Figure 7: (c and d) Aqra Anticline near Bakrman Gorge, with and without interpretation. Location marked by index map. Note that layering in Gercus-Pila Spi (yellow full line) is not conformable to layering in Khurmala (yellow stippled). There are extra folds in the Pila Spi, enabled by the ductile behaviour of the Gercus shale.

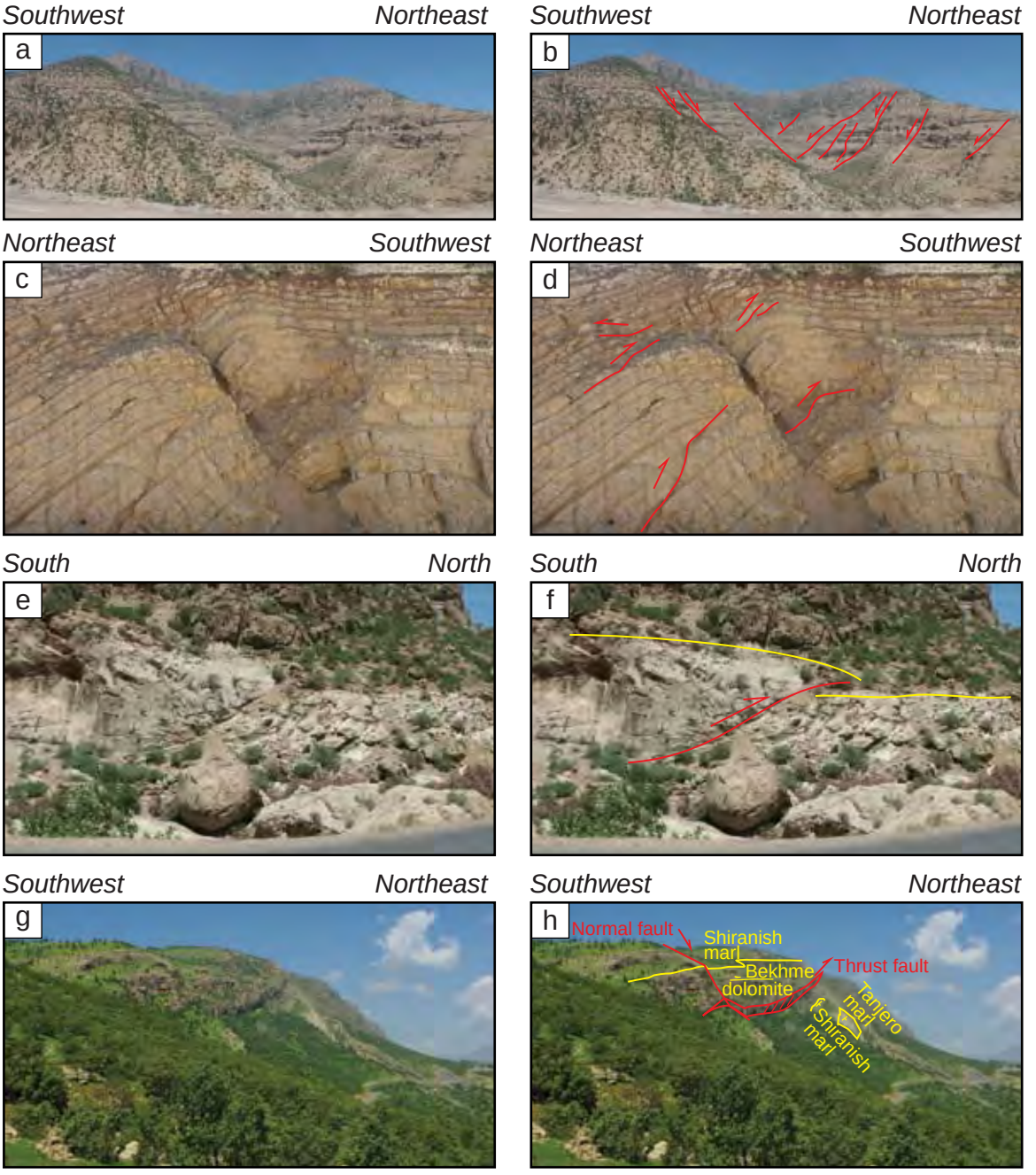

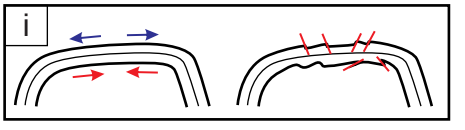

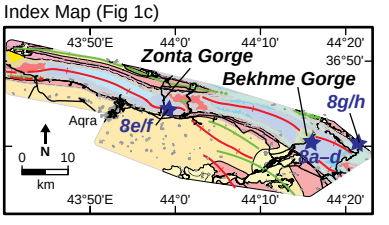

Figure 8: Structural features associated to major folding. (a) Crestal collapse in the core of Bekhme Anticline, uninterpreted. (b) Same, interpreted. Note small offset normal faults (red lines) in well-layered Qamchuqa Formation (Bekhme Gorge, NW face). (c) Smaller internal thrusts in the core of Bekhme Anticline, Sarmord Fm, uninterpreted. Same location as above. (d) Interpreted. Thrusts marked by red. (e) Duplexing related to major folding in Zonta Gorge, uninterpreted. (f) Same, interpreted. Internal thrusts repeating individual layers in Qamchuqa Formation. Internal thrusts: red; layering: yellow. (g) Thrust affecting the northern limb of Bekhme anticline, uninterpreted. (h) Same, interpreted. Yellow marks layering, red marks faults. Note south dipping thrust fault juxtaposing flat layers of Bekhme Dolomite above steeply dipping Tanjero and Shiranish Marls. Note also normal fault dissecting the axis of anticline. (i) Model for orthogonal flexure. Left hand side figure shows extension in outer arc, shortening in inner arc (arrows); right hand side figure shows corresponding structural forms as crestal collapse in outer arc, disharmonic folding and smaller thrusts in inner arc.

On some of the clearly E-W-oriented folds, like the Shaikan Anticline (Figure 1b), there is a set of smaller amplitude superposed folds, which have axial trends oblique to the main axis (Figure 10). These smaller folds form left-lateral *en-échelon* sets arranged along the main E-W trend (idea of Mike Hawkins, ex GKPI). The smaller superposed folds have outcrop expressions. Stereoplots of bedding poles from Central segment in the Shaikan Anticline also suggests a combination of E-W and WNW-ESE axis folds (Figure 10).

Relay of Anticlines

One of the characteristics of major folds in the study area is that they display left-lateral relays on the E-W-oriented segment, right-lateral relays on the NW-oriented segment of the mountain chain. The Bekhme and Aqra anticlines have a clear left-lateral *en-échelon* separation at the Khurmala and deeper levels (Figures 11a to 11d). The map relationship of the Bekhme and Harir anticlines (Figure 1b) is not so straightforward, since at the eastern end the Bekhme Anticline apparently has two periclinal terminations (Figure 1c). However, in the field the northeastern termination of Bekhme and the southwestern termination of Harir are more pronounced and therefore the separation is right-lateral (Figures 2, 11e and 11f). In the wider surroundings of the study area the observed tendency is reinforced by more *en-échelon* configurations. The Harir Anticline, in turn, passes with right-lateral *en-échelon* relay to the Shah Rook Anticline (Figure 1b), which is itself relayed by another set of right-lateral anticlines (Figures 2, and 12). On the E-W trend, the Swara Tikka, the Khoskha and the Dinarta anticlines (Figures 1b and 2) form a set of left-lateral *en-échelon* folds. It is also noted that the left-lateral relays are more apparent, than the right-lateral relays.

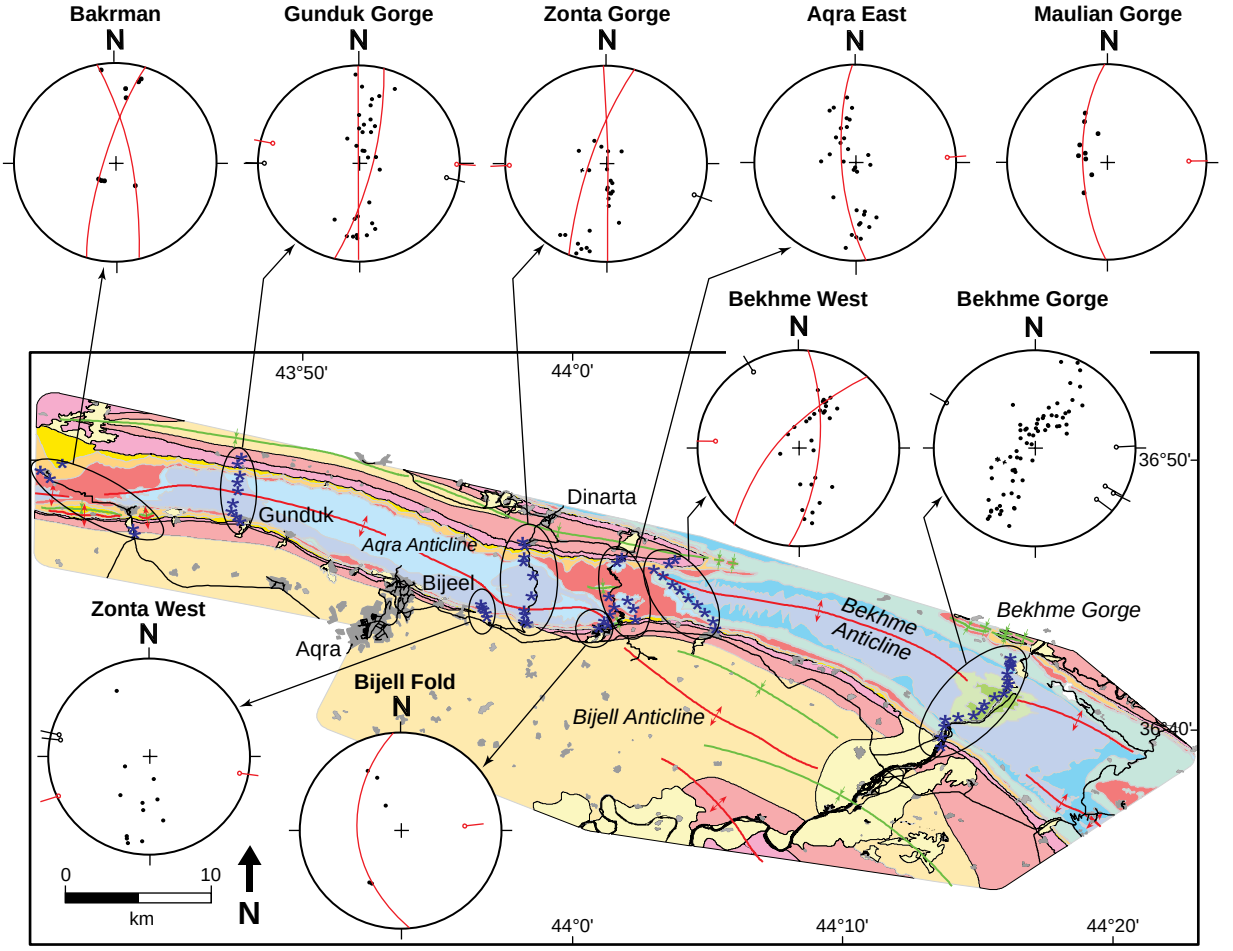

Figure 9: Stereoplots of the measured dips in Aqra and Bekhme anticlines, all equal area, lower hemisphere projections. Measurements marked by blue asterisks on map. Ellipses mark the outcrops used for plot construction. Poles to bedding are marked by black dots. Measured axes marked by black barbed dots. Great girdles marked by red traces. Constructed axes marked by red barbed dots.

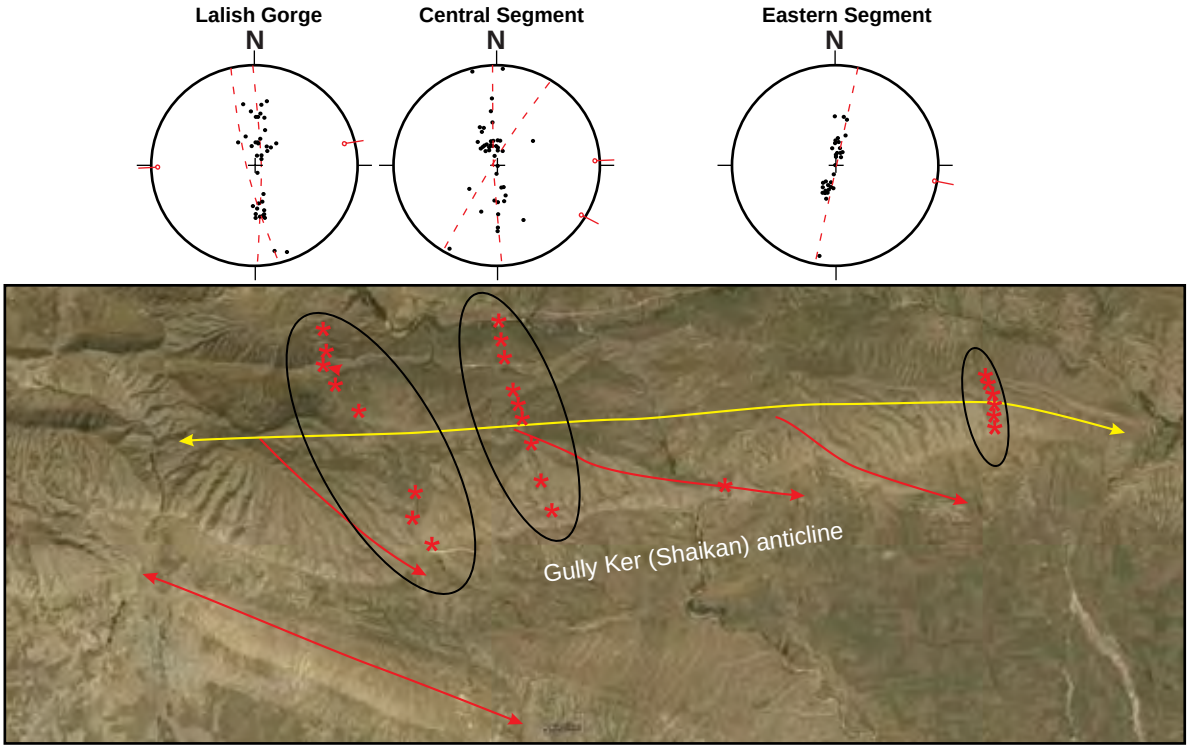

Figure 10: Stereoplots of the measured dips in Shaikan anticline (for locatioin see Figure 1b), all equal area, lower hemisphere projections. Base map is a Google Earth satellite photo. Measurements marked by red asterisks on map. Ellipses mark the outcrops used for plot construction. Poles to bedding are marked by black dots. Great girdles marked by red stippled traces. Constructed axes marked by red barbed dots.

Mapping and dip measurements of Tertiary formations in the southern lowlands reveal folds south of the exposed folds discussed above (Figure 2). Several such folds are indicated by periclinal Pila Spi carbonate ridges (like the Mirawa Anticline) or more resistant outcrops of Lower Fars beds (like the Bardaras and Permam (Sarta) anticlines (Figures 1b and 2). However, divergent dips even in Bakhtiari beds can indicate folds (like the Bijell Anticline, just south of and overthrust by the exposed Aqra Anticline). Most of these folds in the lowlands have a WNW-ESE axial orientation and a left-lateral *en-échelon* arrangement along E-W zones south of the topographic boundary (Figure 12). At least two such zones can be recognised: the Ain Sifni-Rovi-Bijell Zone and the Bardaras-Permam (Sarta)-Safin and Mirawa zones. In this latter zone all the Tertiary anticlines are offset in a left-lateral sense from their respective Mesozoic exposed cores.

Joints

Systematic joints are generally associated with the main folds. These joint sets are parallel, perpendicular to the fold axis and symmetrically oblique to it (Figure 13). Systematic joints are thought to be generated in the incipient phases of folding, during the first layer-parallel compression episodes (e.g. Twiss and Moores, 1992). The parallel/perpendicular elements are tied to extensional cracks, while the oblique couple is imagined as a pair of shear-induced Mohr sets or conjugates. Since incipient compression is generally perpendicular to the future fold axis, all the measurements were back-tilted to horizontal bedding. In this case the acute angle bisector of the conjugate set or Mohr couple can be used to define the incipient shortening directions of the future fold (Figure 14).

When plotted with the fold axes, the back-tilted systematic joint sets show a remarkable rotation (larger composite stereoplots with folded bedding poles and measured axes on Figure 14). In the eastern Bekhme Anticline, the fracture set is symmetrical to a SE-trending fold axial plane. Here the axis-parallel joints can be so dense, that they form layer-orthogonal fracture cleavage. These may somewhat diverge from the mapped axial directions, but the angular difference is minimal. In the

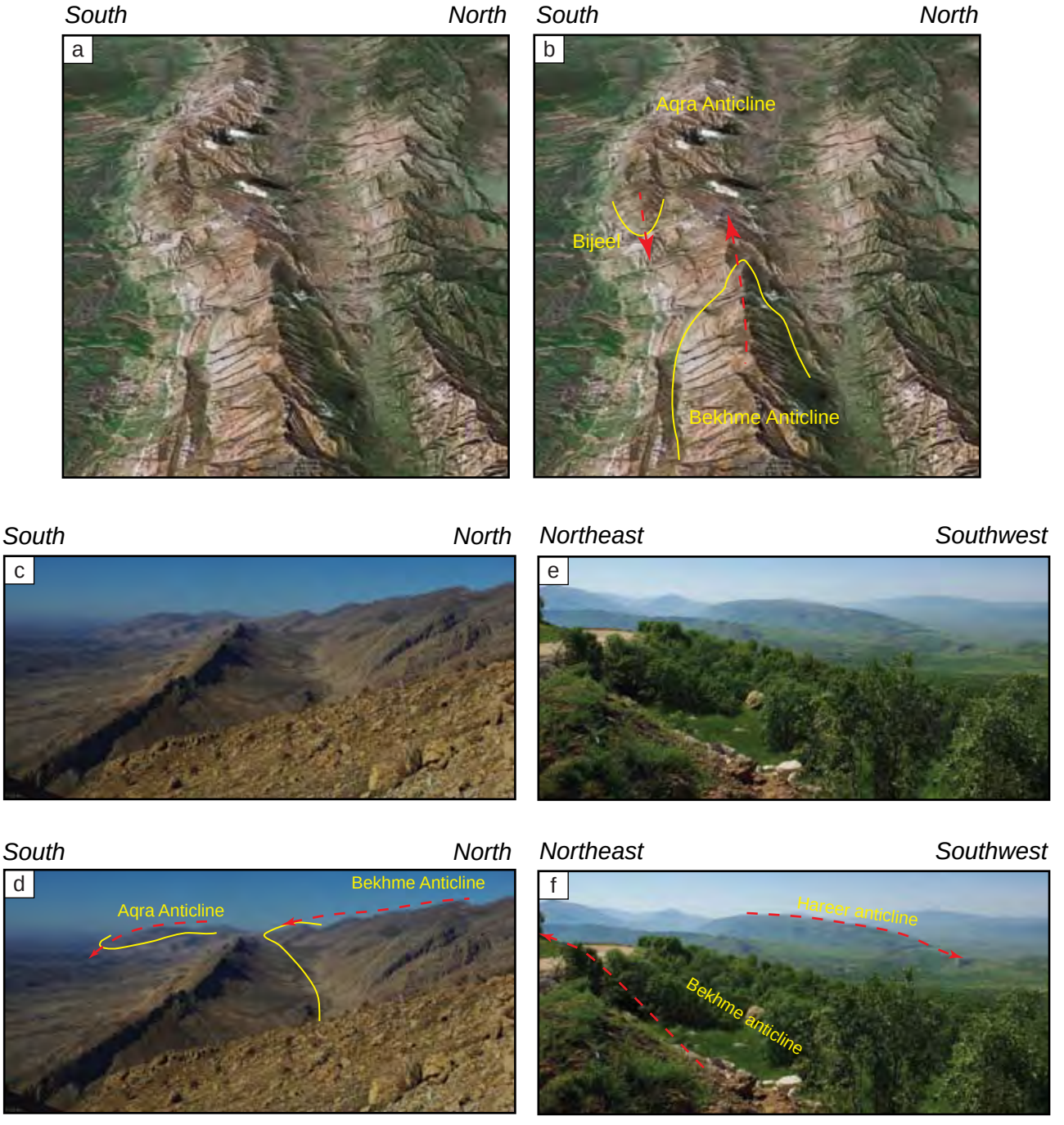

Figure 11: ***En-échelon*** **arrangement of Bekhme, Aqra and Harir anticlines. For names see Figure 1. (a) Satellite view (Google Earth) towards the west of the** ***en-échelon*** **pattern and fold closures of Bekhme (lower part of picture) and Aqra (higher part) anticlines. (b) Interpreted version. Yellow marks bedding; red stippled arrows mark plunging axes. (c) Field photo from Bekhme Anticline (foreground) towards periclinal closure of Aqra Anticline (background). Location marked by red asterisk on insert, photo looking west. (d) Interpreted. Yellow marks bedding; red stippled arrows mark plunging axes. (e) Field photo from Bekhme Anticline (foreground) towards periclinal closure of Harir Anticline (background). Location marked by yellow asterisk on insert, photo looking east. (f) Interpreted. Red stippled arrows mark plunging axes.**

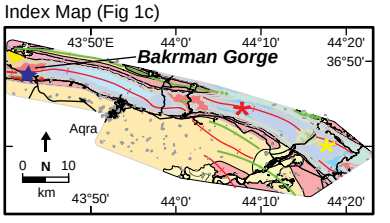

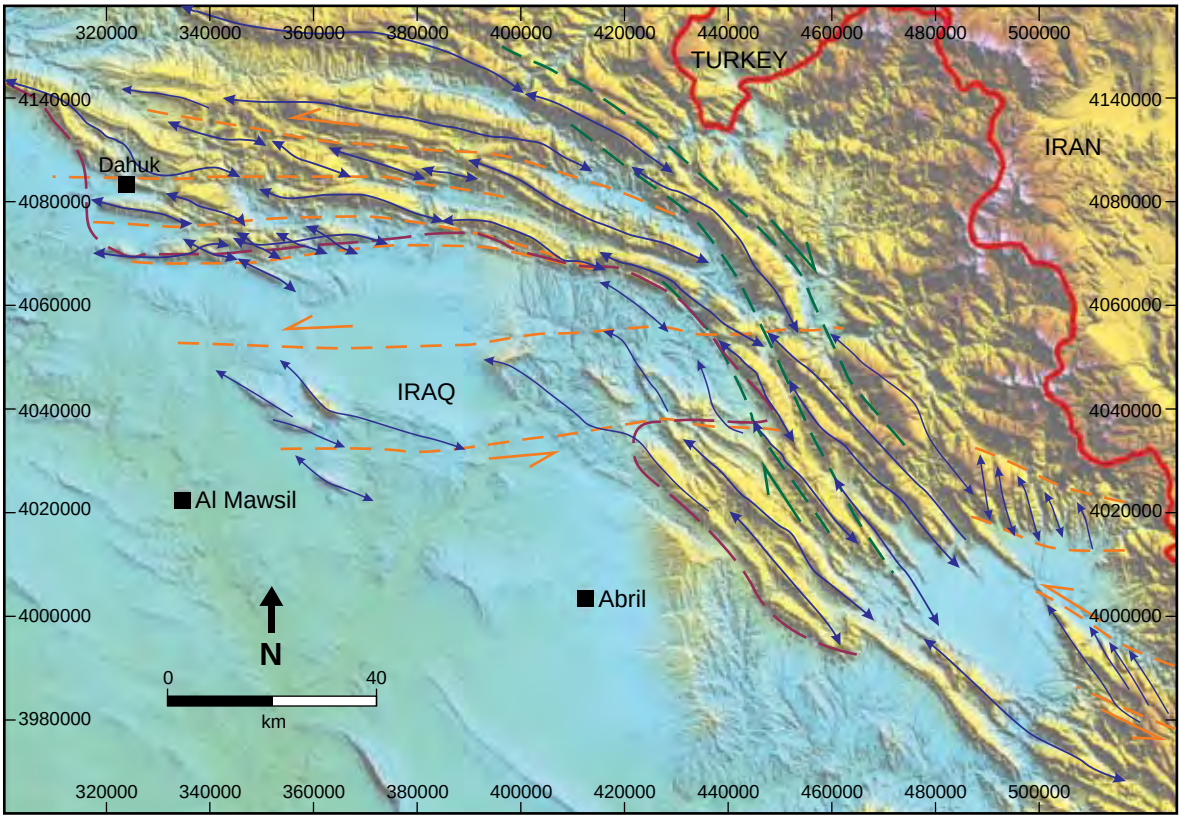

Figure 12: Main tectonic elements of the study area. Tectonic interpretation on NOAA DTM image. The main anticline axes are marked by blue. The interpreted left-lateral shear zones are marked in orange, and right-lateral shear zones in green. Stippled deep purple line marks important blind thrusts zone that explains the topographic break. Note the major change in strike of the structures.

western Aqra Anticline (more precisely the transitional zone from the Bekhme to the Aqra anticlines, including the Zonta Gorge) the interpretation of the fracture set is not so straightforward. We can observe a set symmetrical to a WNW-ESE axis and another one, symmetrical to an E-W axial plane (left larger stereoplot in Figure 14). In the more E-W domain of the western Aqra Anticline (Gunduk Gorge and Bakrman) the plot shows that also here both symmetries can be found. These observations might also support interference of two different shortening episodes, related to folding.

Bitumen Shows

Hydrocarbons often invade the systematic joint sets described above. Bituminous surfaces can even be found in the more ductile marls of the Shiranish Formation (Figures 13a and 13b). It is remarkable that in the Bekhme Gorge the Tanjero Formation above the Shiranish marl does not contain shows, and the Shiranish shows are solely in joints. This fact suggests that the Tanjero Formation and/or the Shiranish Formation was an effective seal, and hydrocarbons were pressure-injected into the otherwise closed fracture system, just at the top of Cretaceous dolomite reservoir section. Another conclusion is that hydrocarbon migration should have occurred after (incipient) fold formation.

Age of Folding

The youngest formation affected by folding is the Upper Miocene and Pliocene Bakhtiari Formation (Figure 2). These young conglomerates fill all the major synforms (Figure 15a). Layering in the Bakhtiari is flatter than in the adjacent Upper Fars: a progressive unconformity (onlap of the uppermost Upper Fars and Bakhtiari during fold growth) is observed (Figure 15b). The onlap associated with fold growth may be heterochronous, which is not unique in the Zagros (see Homke et al., 2004).

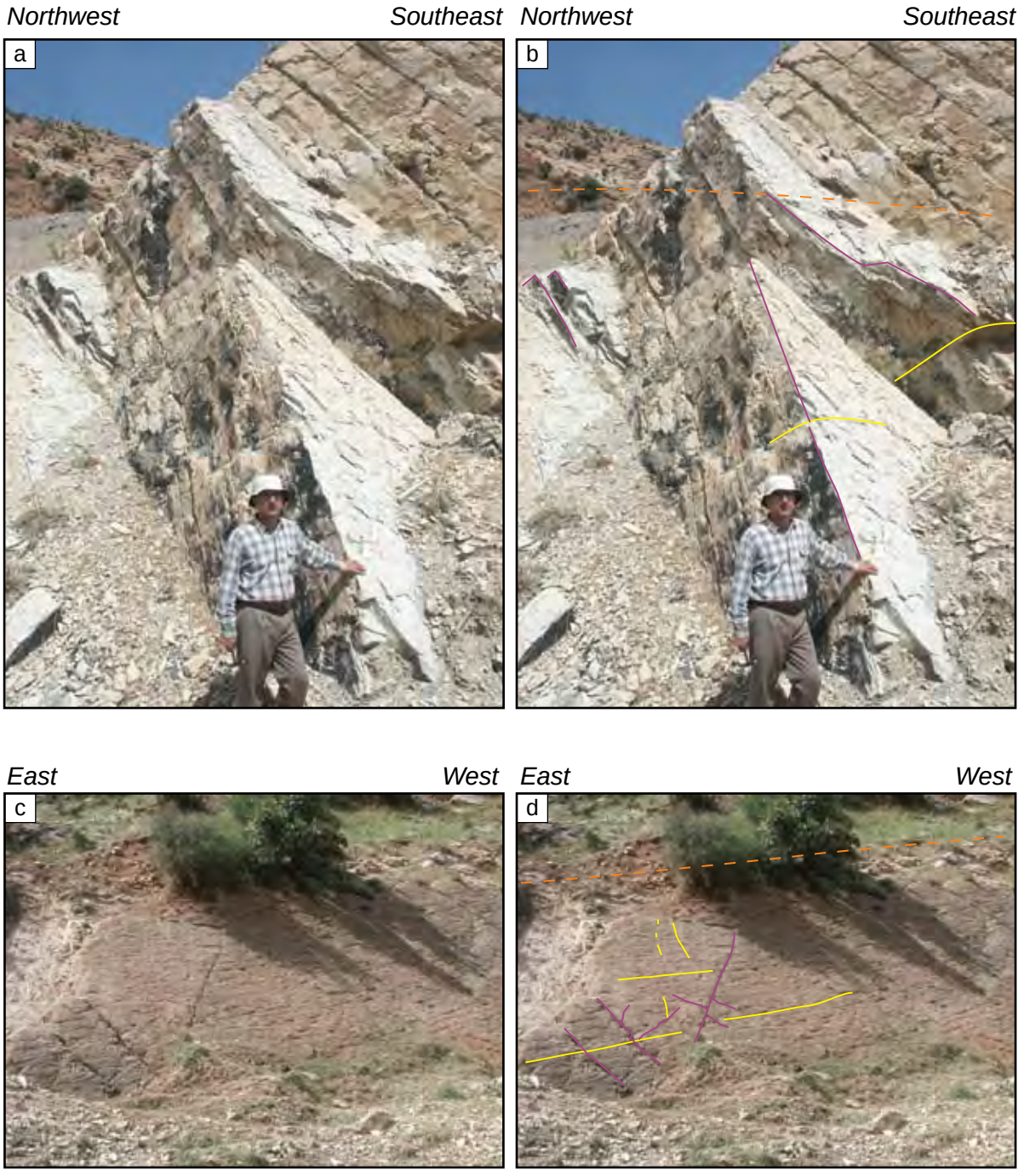

Figure 13: Systematic joints associated to folding. (a) Road cut at southern slope of Bekhme anticline, uninterpreted. Location marked by red asterisk in insert map. (b) Same, interpreted. Note axis- parallel/perpendicular (yellow) and oblique (violet) sets in Shiranish Marl. Fold axis is marked by orange stippled line. The acute angle bisector is perpendicular to the fold axis. Note that bitumen (oil) migrated along these surfaces. (c) Fractured Pila Spi limestone layer along the Bijell-Dinarta road. Location marked by green asterisk in insert map. (d) Same, interpreted. Acute bisectrix is perpendicular to fold axis.

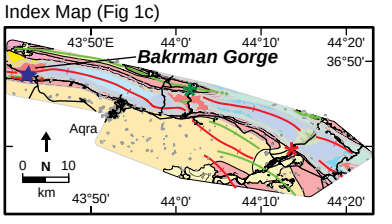

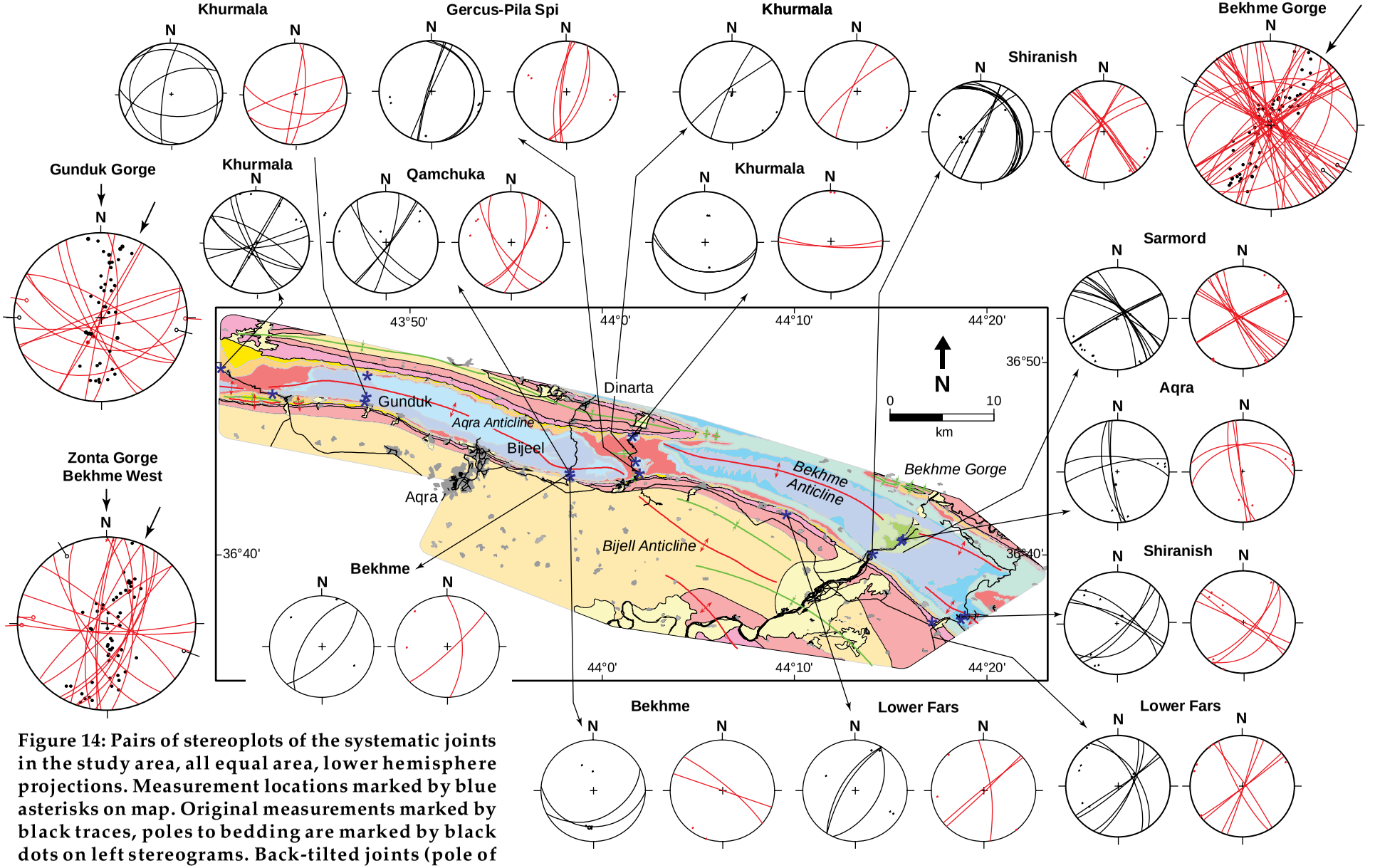

Figure 14: Pairs of stereoplots of the systematic joints in the study area, all equal area, lower hemisphere projections. Measurement locations marked by blue asterisks on map. Original measurements marked by black traces, poles to bedding are marked by black dots on left stereograms. Back-tilted joints (pole of bedding to centre) are marked by red traces on right stereograms. Bigger stereoplots integrate re-tilted joints of larger areas. Poles to bedding and measured axes from same areas are copied on same plots as black dots and black barbed dots. Interpreted bisectrices are markedas black arrows on outer periphery of plots.

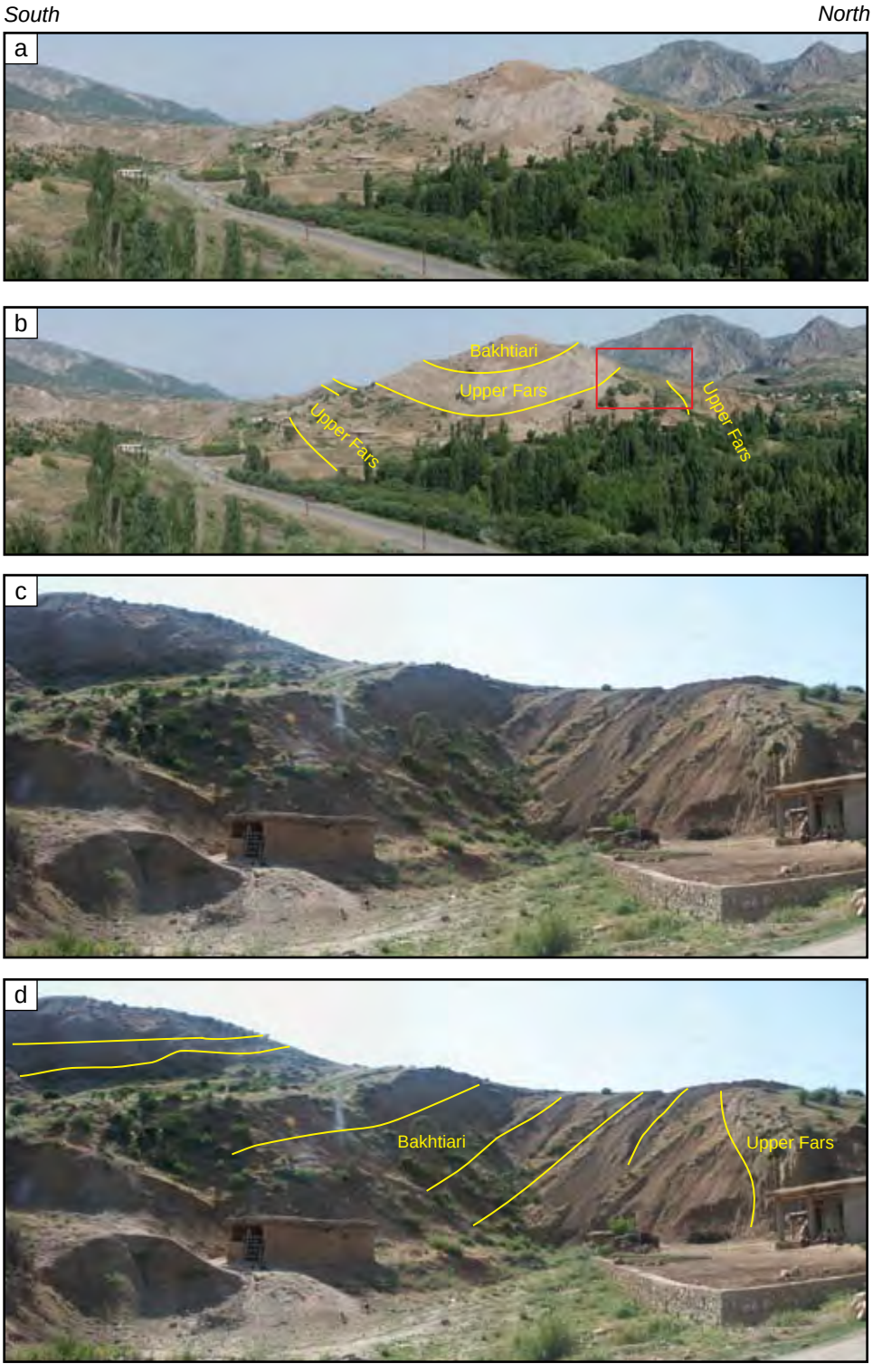

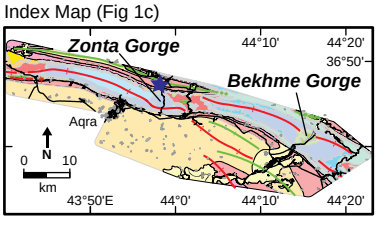

Figure 15: Gradual onlaps in Upper Fars-Bakhtiari syncline. (a) Syncline within Upper Fars and Bakhtiari formations. Picture taken to the west of Dinarta. Location marked on insert map. (b) Same, interpreted. Yellow marks layering. Note dip difference between older and younger formations. Red cage marks location of C, D. (c) Blow up of northern limb. (d) Same, interpreted. Continuous dip change within Upper Fars and Bakhtiari formations. Younger layers of Bakhtiari onlap the folded/tilted older ones.

Map-scale Thrusts

Observed Thrusts

Several thrust exposures were found at the southern limbs, and one at the northern limb, which suggest that thrusts underlie the limbs of major folds. Here two exposures are shown to illustrate the nature and appearance of these thrusts. The best mappable thrust is located at the southern exit of the Zonta Gorge (Figure 1c), where steep, subvertical Mesozoic formations are thrust on top of overturned (down to 40°) Upper Fars and Bakhtiari formations (Figures 16a and 16b). The thrust is also evidenced by a gradual cut-off of younger formations against the Bakhtiari towards the north (Figure 16c).

The northern limb of the Bekhme Anticline hosts a thrust fault cutting through Mesozoic formations (Figures 1c, 8g and 8h). It superposes a normal, flat-lying succession of Bekhme-Shiranish-Tanjero beds on top of steeply north-dipping Shiranish and Tanjero marls of the northern limb. Thrusts on both flanks of anticlines are common. Analogue experiments suggest that they are more a rule than an exception (e.g. McClay and Whitehouse, 2004, their figure 3a).

Thrust faults generally ramp into ductile clays intercalated in the Tanjero, Gercus, and Lower Fars formations. These form detachment levels within the stratigraphic sequence. Ductile flow of material within a detachment zone might also be responsible for the different dips of strata on either side of the detachment.

Geoseismic Section

A geoseismic section was constructed based on proprietary seismic data and on surface dip measurements (Figure 17). This section shows that folds in the less deformed lowland originate from the inversion of earlier normal faults that define fault-bound wedges. These wedges are then pushed up against the faults to form the box folds observed at surface. As a rule, one of the confining faults has a greater offset, but this is not necessarily the southern one. In the Bekhme and Aqra anticlines, the top-to-the-north thrust seems to be generally more important. This fault detaches below the Triassic Kurrachine dolomite (base of violet layer on Figure 17), most probably in an evaporite. Also as a rule, the same horizon is the upper detachment of a duplex of Palaeozoic rigid units, which have yet a deeper lower detachment (Hormuz Salt?). This duplex is generally south-vergent, and may be the equivalent of the Main Frontal Fault. The top-to-the-north surface thrusts act as a hanging wall duplex above the leading edge of the Palaeozoic duplex.

Fault Measurements

General Methods

Wherever possible, fault attitude and fault-slip measurements were performed. Data were plotted for each outcrop, in present attitudes and with bedding attitudes 're-tilted' to horizontal (Figure 18). Special care was taken when overturned beds were encountered. We separated faults found in the Neogene Lower and Upper Fars, and Bakhtiari formations from faults found in Palaeogene and Cretaceous rocks (Figures 18a and 18b). No major difference is seen in the fault pattern. The more numerous observations in older rocks are related to the better preservation of faults in brittle carbonates, than in softer siliciclastics and shales.

Individual outcrops do not yield sufficient data to perform a meaningful numerical tensor analysis for each outcrop, like e.g. Navabpour et al. (2008). Another difficulty is that the time of formation of individual faults or striations could not be fixed. In some outcrops, it seemed that fault timing in a re-tilted position makes more sense; in other outcrops it seemed more logical that faults were formed in the present (often steeply dipping) bedding position. This is a problem, since even the youngest beds may be overturned, and all evidence suggests that faults were created during the folding phase(s). Since no direct proof for formation time of faults could be given, we decided not to perform calculations on amalgamated sets, or to deal with average stress tensor directions, but to present just the data and to draw first-hand conclusions.

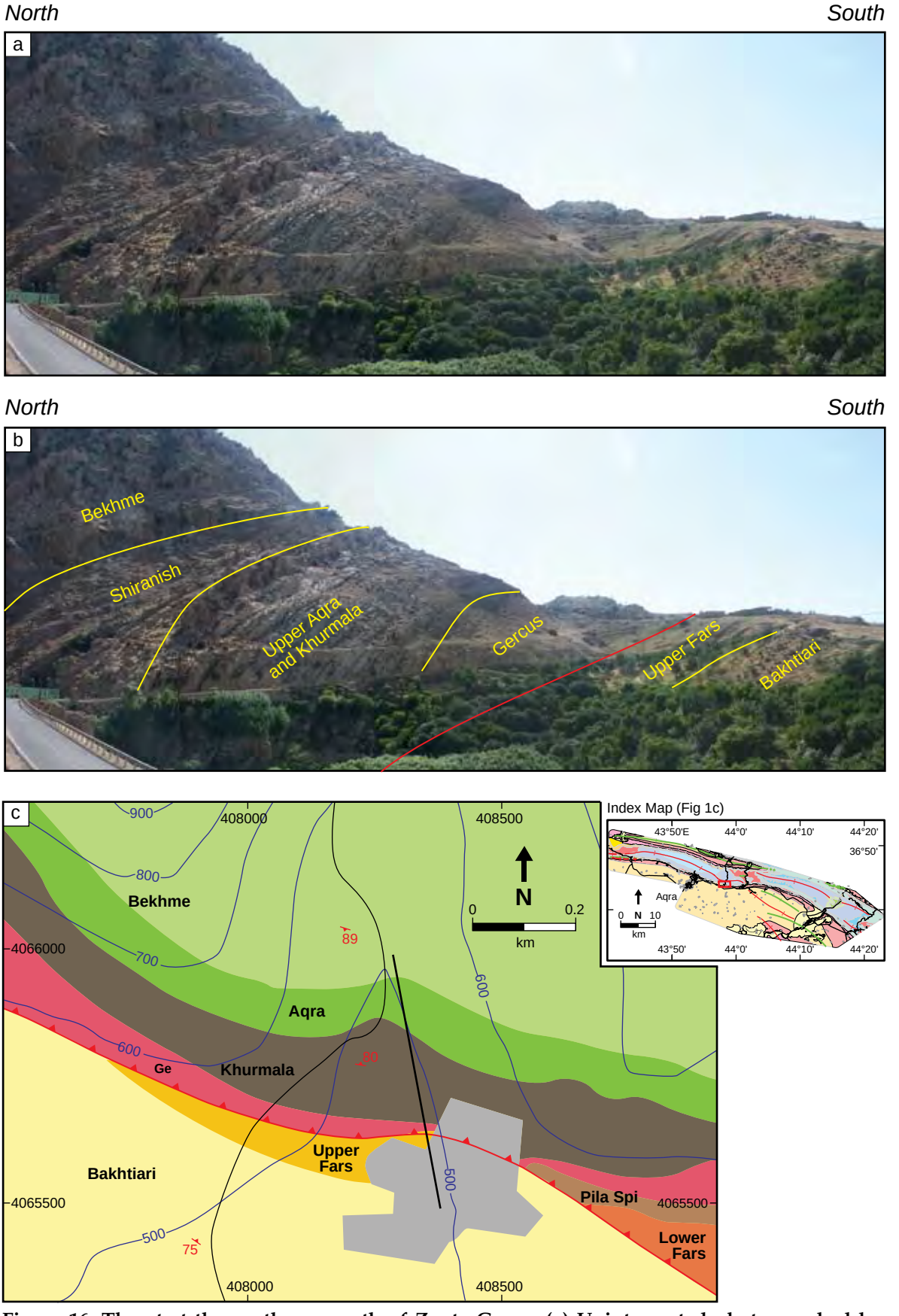

Figure 16: Thrust at the southern mouth of Zonta Gorge. (a) Uninterpreted photo, marked by black line on C. Location marked by red box on insert map. (b) Same, interpreted. Khurmala and Gercus formations are thrust upon Upper Fars and Bakhtiari. All beds are overturned. Overthrust is younger than Bakhtiari. (c) Geological map from the southern mouth of Zonta Gorge. Contour interval = 100 m. Note the cut-off of Pila Spi Limestone by the thrust surface (red). This surface is slightly offset by later strike-slip faults.

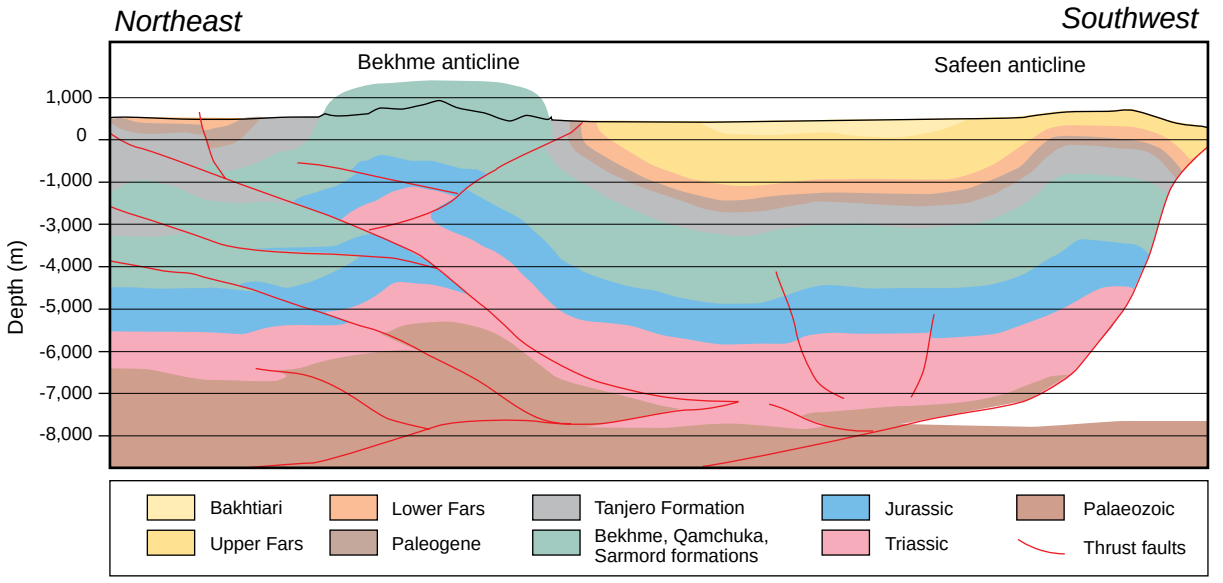

Figure 17: Geoseismic section across Bekhme anticline, based on surface dip measurements and proprietary seismic section transformed to depth. Location on Figure 1.

Separation and Analysis of Measured Faults

After plotting individual fault data, we first separated sites that were least tilted. We considered (especially in case of Neogene) that these faults were only slightly rotated after being active. A manual separation into potential synchronously active fault families was performed on this data (Figure 19). Subsequently, we analysed the fault sets with large bedding dips and analysed if in their present position the faults fitted any of the fault families defined in the less tilted strata. Finally educated guesses about the potential shortening directions were made. Unfortunately, no superposed striations were found, and therefore no clear chronological relationship between the identified fault patterns could be established.

We tried to group the data around two major regions: the surroundings of Bekhme Gorge and the surroundings of Zonta Gorge. These two areas also correspond to the somewhat differently oriented fold segments (Figure 9). Both in the younger and older rocks we can observe thrusts, normal faults and strike-slip faults of similar attitudes and offsets.

Three sets of thrusts might be observed (Figure 19): ones possibly generated by NE-SW compression; others possibly generated by N-S compression. Since the striations do not form distinct clusters, it seems that there is a gradual transition between these shortening directions, and that this deformation affected the whole study area in a homogenous way. The third set of thrusts was possibly generated by a NW-SE compression that apparently did not produce map-scale structures. Even more interesting, both western and eastern sectors show hints of NW-SE shortening, also in a quite homogenous way.

Two strike-slip fault sets might be differentiated: one with N-S right-lateral and ENE-WSW left-lateral faults, possibly created by NE-SW compression and NW-SE extension, and another one with NE-SW left-lateral and NW-SE right-lateral faults, possibly created by N-S compression and E-W extension. E-W left-lateral faults might belong to the first stress field. Some E-W right-lateral faults might belong to NW-SE compressional field.

Normal faults were also observed and measured. There is one set of crestal collapse normal faults (NE-SW extension) in the core of the Bekhme Anticline. There are two other sets of normal faults: ones generated by E-W extension and others generated by NNW-SSE extension. This latter set might have been active in the pre-folding phase.

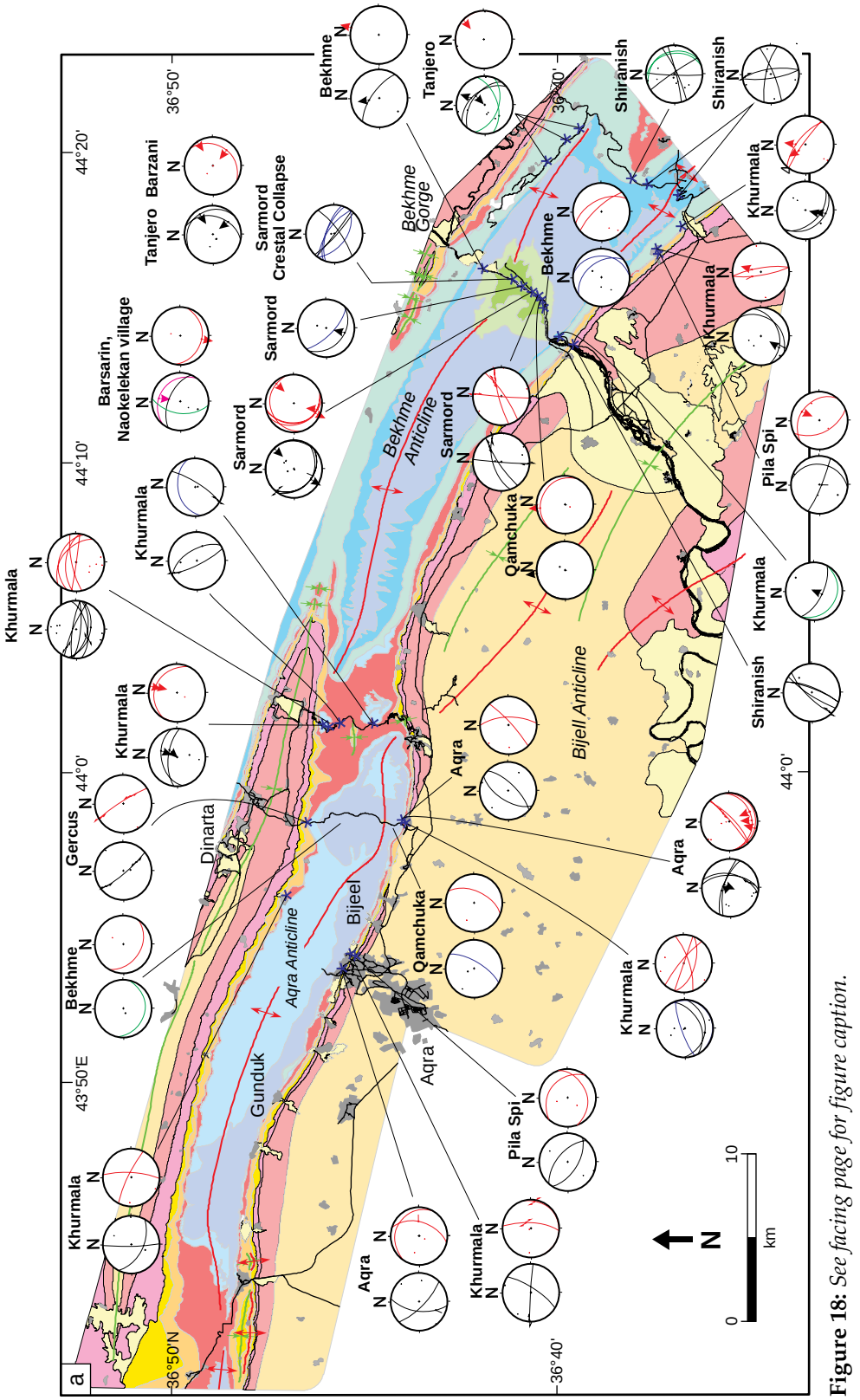

Figure 18: *See facing page for figure caption.*

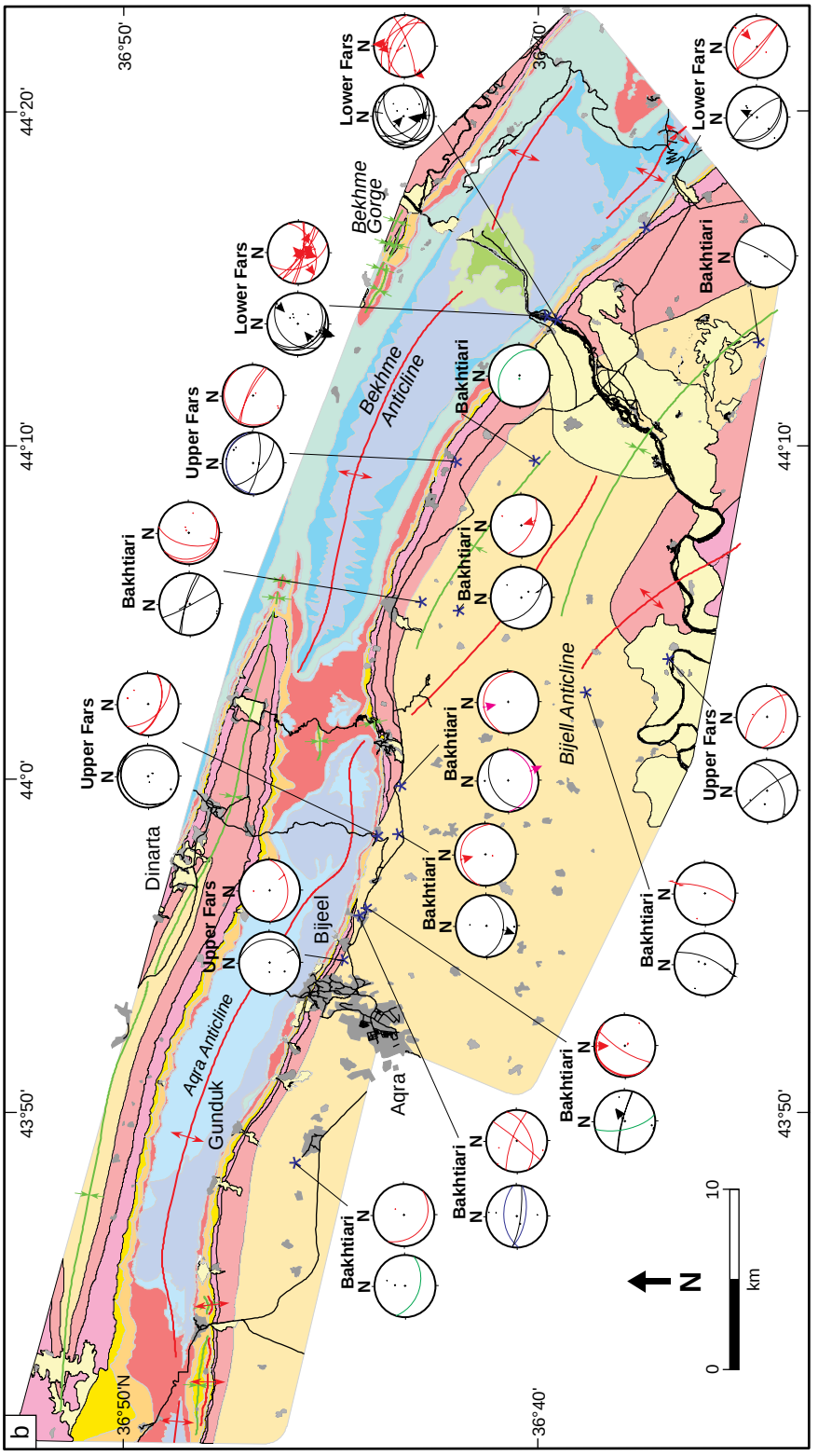

Figure 18: Pairs of stereoplots of the measured faults in the study area, all equal area, lower hemisphere projections. Measurement locations marked by blue asterisks on map. Measured formation name indicated above each plot. Original measurements marked by black traces, poles to bedding are marked by black dots on left stereograms. Conventional slickenslide lineation marks: arrow to internal part= thrust fault; to outer part= normal fault, right- and left-shear arrows= right- and left-lateral strike slip movement. Some more important thrusts (green) and normal faults (blue) without slickenslides, but with certain offset were also plotted. Back-tilted faults (pole of bedding to centre) are marked by red traces on right stereograms. (a) Stereoplots measured in Palaeogene and older formations. (b) Stereoplots measured in Miocene and younger formations.

There seems to be no substantial rotation between the faults and related potential stress fields of the eastern ("Zagros trend") and western ("Taurus trend") regions, although some minor angular difference between the two regions is detected.

Bitumen and Faults

Bitumen staining is very often found along thrust faults in different Mesozoic formations. Fault surfaces with fault gauge breccia, or non-filled, displaced thrust fault cavities (dilatation jogs) were also filled by bitumen (Figures 20a and 20b). This suggests that thrusting was synchronous to, or followed by hydrocarbon migration.

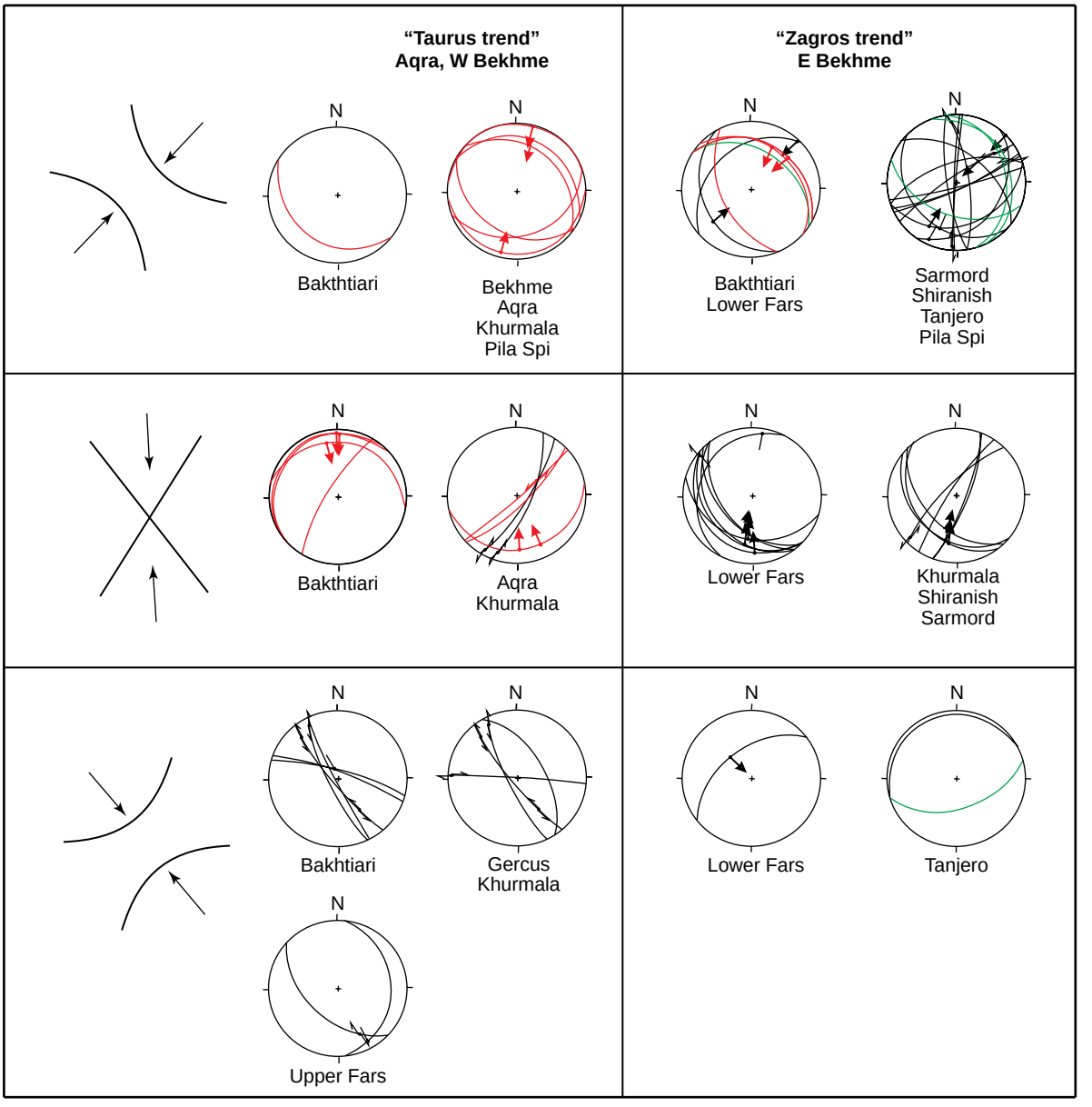

Figure 19: Separation of the fault data into sub-families. Method described in the text. The faults are separated into two regions (i.e. two columns): Zagros trend (surroundings of Bekhme Gorge) and Taurus trend (surroundings of Zonta gorge). Three "phases" may be separated: a NE-SW; a N-S; and a NW-SE compression dominated one. Data recorded on Neogene and younger (left stereoplot) and on Palaeogene and older (right stereoplot) are also differentiated. Black and green signs indicate data in measured (present) position; red signs indicate re-tilted data (bedding to horizontal) For all symbol explanations see Figure 18.

CONCLUSION ON STRUCTURAL OBSERVATIONS

Structural Pattern in Kurdistan Region of Northwest Iraq

In our study area there are several main characteristics for the deformation pattern. The most obvious is the change of trend of the major folds from the NE-SW "Zagros trend" to the E-W "Taurus trend" (Figure 1a, b). These segments are also different, because there are systematic right-lateral *en-échelon* relays along the Zagros trend, and left-lateral *en-échelon* relays or interference folds along the Taurus trend. Several sets of left-lateral *en-échelon* folds are found in the southern lowlands, along E-W-oriented zones.

Like other authors, we also propose that the marked topographic rise corresponds to a top-to-the-south-southwest blind thrust, that carries the whole Mesozoic section (Figure 12, 17). The smaller emergent thrusts are on one hand too steep, and on the other, they have variable throw, and therefore cannot be the basic reason for the topographic difference (Figure 17). The folds are accompanied by conjugate thrusts that may create larger offsets and even overturned layers in Tertiary sediments.

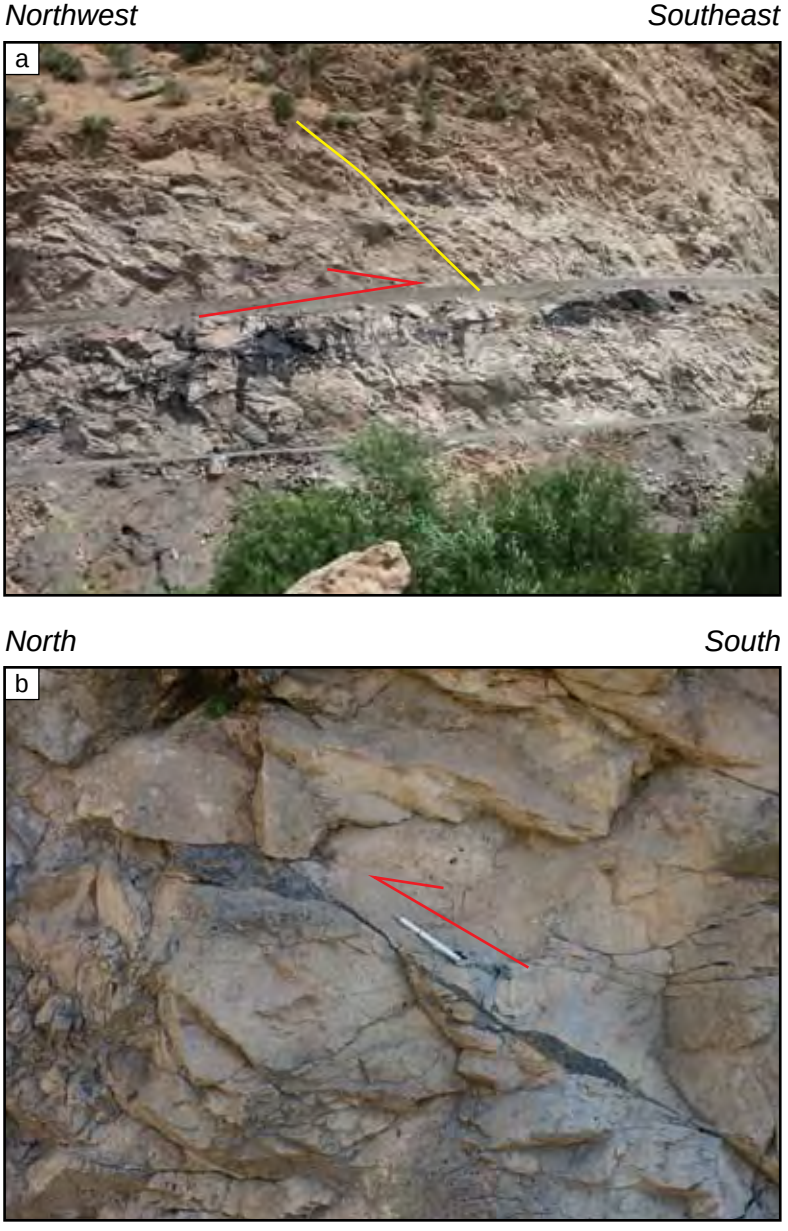

Figure 20: Bitumen in faults. (a) Big fissure leaking oil/bitumen at the southern entry of Bekhme Gorge, along road, opposite bridge. Location given by red asterisk in insert map. Note that fissure obliquely transects layering (yellow). (b) Young thrust fault filled in the separated cavities by bitumen in Zonta Gorge. Location given by blue asterisk in insert map.

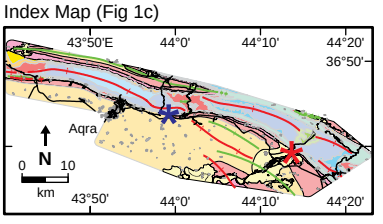

However, these are possibly inverted earlier normal faults. Such structures are also present beneath the lowland (Figures 12 and 17). The change in shape of the topographic rise may reflect a change in the position of this blind thrust (Figure 12). It is suggested that this is an inherited fault, linked to the original shape (or earlier structures) of the Arabian Margin.

Based on our section (Figure 17) the blind thrust may create duplications within the Palaeozoic section and may have its upper detachment at a Permian or Triassic evaporitic horizon. The conjugate thrusts entwining the major anticlines may rise from that lower detachment and run into the Palaeogene Gercus or Neogene Lower Fars shales. The top-to-the-north thrusts within the Mesozoic section may be interpreted as hanging-wall backthrusts to the lower top-to-the-south blind thrust.

Sequence of Deformation Events

A pre-folding NE-oriented shortening, coupled mostly with top-to-the-southwest shear, can be documented in both the Zagros and Taurus trends. This early deformation is however, gently counter-clockwise rotated in regions of the Taurus trend.

Major folds are present in both segments, with their corresponding systematic joint sets, oriented according to the fold axis (Figure 14). These major folds do not necessarily form at the same time. While there seems to be a unique phase of joints in the Zagros trend folds, there also seems to be a superposition of a gently counter-clockwise-rotated NE-SW symmetrical and a N-S symmetrical joint set along the Taurus trend.

Because the northern structures are deeper incised and expose deeper stratigraphic levels than the southern structures, it seems they were subject to longer erosion, and therefore it is probable that the folds and thrusts propagated towards the southwest. Stratigraphic sequences trapped in synclines between the different anticlines allow age determinations in the Iranian Zagros (Hessami et al., 2001; Homke et al., 2004), which also indicate a southeast thrust propagation. Hessami et al. (2001) suggested that convergent deformation may have started in Eocene, but certainly from Early Miocene and propagated SW in the Pliocene. Our study area falls approximately in their Middle Miocene–Pliocene zone of convergence, which is also supported by our observations (Figure 15).

Fault-related Deformations

Faults can be grouped in deformation events created by three main compression directions. Even the youngest Bakhtiari Formation records many of these faults, hence deformation is younger than Middle-Late Miocene. The relation of faults and folds is controversial: some fault patterns appear as pre-folding, others appear as post-folding patterns. There might even be faults that were created in an interim stage of folding.

NE-SW compression can create conjugate NW-striking thrust faults, shear zones, as well as N-S-oriented right-lateral and ENE- to E-W-oriented left-lateral faults.

N-S compression can create conjugate E-W-striking thrusts, shear zones, as well as NW-SE right-lateral, NE-SW left-lateral strike-slip faults and N-S-oriented normal faults. The latter may gently cut up the anticlines in a transverse direction.

In some recorded data, a gradual transition between NE-SW compressive and N-S compressive directions is evident.

An enigmatic NW-SE compression is also present, apparently not creating map-scale structures. NE-striking conjugate thrust faults, together with N-S-striking, left-lateral and E-W-striking, right-lateral faults and eventually NW-oriented normal faults may be created by this compressional stress field.

Although the few collected fault data do not allow a relative timing of events, other evidence points to a temporal change from NE-SW compression to N-S compression. Shortening preceding folding appears NE-oriented; thrusting during or after folding appears oriented from NE-SW to N-S.

The observed sequence of deformation is very similar to the sequence of events in the Iranian part of Zagros (Lacombe et al., 2006; Navabpour et al., 2007, 2008). Lacombe et al. (2006) set up different models, with and without strain partitioning, to explain the observed deformation pattern and sequence. Navabpour et al. (2007) recorded most of their data within the High Zagros Belt, around the Main Recent Thrust (which is a principal right-lateral displacement zone providing strain partitioning), yet they found the same events with similar stress directions. Navabpour et al. (2008) suggested that in Lurestan (Figure 1a) the NE-SW compression before folding was acting in Early Miocene, the main folding occurred in Middle-Late Miocene. Some NNE-SSW compression after folding happened in Late Miocene–Pliocene and the change of stress field to N-S compression occurred in Pliocene. They also evidenced a NW-SE compression after main folding.

Kaymakci et al. (2010) collected and analysed fault slip data on both the Arabian Platform and on the allochthons of the Tauride segment. In the Turkish part of the Arabian Platform they interpreted their data as having a (1) Palaeocene–Eocene NE-SW extension; 2) Eocene–Early Oligocene ENE-WSW compression; (3) latest Oligocene–Middle Miocene NW-SE extension; (4) Middle Miocene–Pliocene NNW-SSE compression; and (5) a Middle Pliocene NNE-SSW to NE-SW compression. Evidently, our data set is not as refined as theirs, and absolute timing of the structural events in our study region is not yet possible. However, in their youngest data set they have the same thrust directions as observed by us, smeared between NE-SW and N-S. Therefore we propose that both areas, the Zagros and Taurus trends, underwent the same deformation, that may be interpreted in different ways, but that has very similar signatures.

DISCUSSION ON OROCLINAL BENDING *VERSUS* PRE-FORMED BUTTRESS

Fold orientations, together with their linked fracture sets, diverge in the Zagros and Taurus segments of our study area. There are basically two explanations for this change in structural orientation: (1) a rotation of the western or eastern segments (oroclinal bending); or (2) moulding on the buttress of the Arabian Platform edge.

Oroclinal bending of the "Taurus trend" is not probable, because neither westward increase in thrusting, nor increased topographic uplift relative to eastern areas is seen. Preliminary palaeomagnetic results seem to contradict any large rotation in the Mardin High (Figure 1a) region, i.e. the Taurus trend part of the mountain chain (Peynircioglu, 2010). Sparse fault data also suggest that the two different segments did not suffer major relative rotation (see e.g. the NW-SE shortening and the minimal angular difference in these deformation patterns between the two sectors).

Moulding suggests that structures are oriented by the pre-existing buttresses. That system does not create space problems and implies that local orientation closely follows the shape of the Arabian Platform (Figure 12).

DISCUSSION ON STRAIN PARTITIONING *VERSUS* SUCCESSION OF DEFORMATION PHASES

Based on GPS and earthquake focal mechanism data, an overall Recent N-S convergence of the Arabian Plate towards Eurasia is evident (Blanc et al., 2003; Vernant et al., 2004; Lacombe et al., 2006). In northern Iraq the direction of convergence is NNW-SSE, rather than true N-S. This Eurasian-Arabian plate convergence vector is thought to be the reason for all observed structures (e.g. Allen et al., 2004). Plate tectonic reconstruction (Cochran, 1981; McQuarrie et al., 2003) suggests that the rotation of Arabia *versus* Eurasia gradually changed in time. This resulted in a ca. NE-SW trending shortening during earlier phases of convergence (Oligocene to Early Miocene) gradually shifting to N-S convergence in Late Miocene–Present.

Several authors have suggested strain partitioning to explain the different shortening directions observed mainly in Iran (e.g. Talebian and Jackson, 2002; Blanc et al., 2003; Allen et al., 2004; Lacombe et al., 2006; Navabpour et al., 2008). In that model the southern foreland should accommodate only NE-SW shortening, while the Main Recent Thrust should accommodate an important right-lateral shear (Figure 1a). In Lurestan and Fars this concept works: with rare exceptions the present-day deformation patterns of the two different parts (SW of Main Recent Thrust and NE of it) obey this rule (e.g. Navabpour et al., 2008, their Figure 4). However, adaptation of this concept to the Kurdistan Region of Iraq raises some problems.

1) **The exact extent and potential northward termination of the Main Recent Thrust**
This fault seems to splay off and diminish in offset towards the Kurdistan Region of Iraq (Figure 1a). It may extend until the Yüksekova Basin of southeast Turkey (stippled portions of the Main Recent Thrust on Figure 1a), but its surface expression is diminished. Along this hypothetic portion the earthquakes (big enough to yield a focal mechanism) become quite rare (e.g. Heidbach et al., 2008; Talebian and Jackson, 2004, Figure 1a). Only one earthquake with focal mechanism is found east of our study region. If the Main Recent Thrust ends north of the Kurdistan Region of Iraq (dense line on Figure 1a) this might explain the presence of mostly NE-SW convergence to the south of the Main Recent Thrust ("Zagros trend") *versus* the mainly N-S convergence in the region where its effects as right-lateral fault are diminished ("Taurus trend").

2) **Superposed structures**
If strain partitioning works in our region, then one should expect *only* NE-SW shortening in the block SW of the Main Recent Thrust and only N-S shortening in the "Taurus trend", where the Main Recent Thrust does not exist. However, our data suggest that in both areas both NE-SW and N-S convergent structures are present. The existence of such structures in the "Taurus trend" seems to be the more problematic, since there is no obvious reason to explain structures related to NE-SW shortening. The present-day and Neogene plate convergence was perpendicular to this trend; the present stresses are also perpendicular to the trend.

3) **Different tectonic phases**
This is in fact the same problem as in point 2. In different parts of Zagros (Fars: Lacombe et al., 2006; High Zagros: Navabpour et al., 2007; Lurestan: e.g. Navabpour et al., 2008; and our study area) the same brittle stress patterns were found with very similar timing. Both NE-SW and N-S compression were recorded and these were clearly linked to different episodes (Lacombe et al., 2006; Navabpour et al., 2008). Moreover, these different stress episodes were found both in the "Zagros trend" and in the "Taurus trend". Rigid body rotation might be a solution to this problem (i.e. the block recording deformation rotates under a stable external stress field), but Navabpour et al. (2008) and also our study did not reveal major block rotation.

Navabpour et al. (2008) suggested that the zone of deformation partition (i.e. the active major right-lateral shear zone) shifted south with time. In early phases, when the partitioning boundary is far towards the north, the whole "southern" region is subject to NE-SW compression. When the partitioning boundary moves to the south, its closer vicinity experiences N-S shortening, while the region to the south of this new boundary still experiences NE-SW shortening.

Translating that concept to our study area, in early phases the precursor main right-lateral shear zone was much more to the north, in Iranian territory. In this episode, the whole Kurdistan Region of Iraq, including the "Taurus trend", experienced NE-SW shortening. When the right-lateral shear zone shifted to its present, partly hypothetical, location along the Iranian-Iraqi borderland, the "Zagros trend" experienced N-S compression with right-lateral shear. Since the Main Recent Thrust ends before reaching the "Taurus trend", this area also experienced N-S compression.

An alternative to the above solution is that the tectonic activity along the Main Recent Thrust was not continuous in time, neither was its lateral extent constant. This would mean an alternation of the two compressional phases. In periods when the Main Recent Thrust was inactive, we expect N-S compression in the whole area. In periods when the Main Recent Thrust was active, the region

south of it experienced NE-SW shortening, while there was right-lateral shear along the Main Recent Thrust. This concept is not probable, because once a well-established fault system becomes active it will create a weakness zone that is unlikely to be left inert in a subsequent deformation episode.

Another alternative is that the different recorded tectonic phases do represent different convergence periods of Arabia against Eurasia. Early (to Middle) Miocene NE-trending underthrusting of the Arabian Platform would create ortho-structures parallel to the NW-SE margin, while the same deformation would induce shortening coupled with left-lateral shear and *en-échelon* structures on the EW-oriented "Taurus trend" margin and in the southern lowland (Figure 21a). N-S shortening would be related to latest Miocene–Pliocene structures. This would create ortho-structures in the "Taurus trend", while the same phase would generate right-lateral shear and superposed folding along the "Zagros trend" (Figure 21b). Although that concept does not exclude strain partitioning (especially in Late Miocene–Pliocene), it is not a necessity either. This concept could explain the observed features, although it is likely, that some sort of strain partitioning existed in the Zagros from early deformation phases onwards (Navabpour et al., 2008).

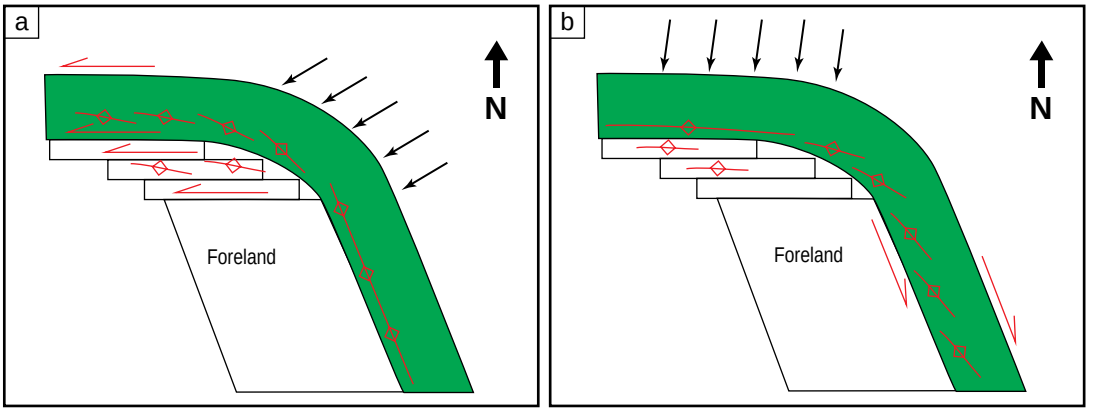

Figure 21: Models for the structural development of Kurdistan Region of Iraq. Green stripe marks the thrusted-folded part of Zagros. Black arrows indicate main directions of Eurasia-Arabia convergence. (a) Earlier NE-SW convergence direction generates "head-on" structures in NW-oriented segments and E-W oriented *en-échelon* structures and left-lateral shear on E-W oriented segments. (b) Recent N-S convergence direction generates "head-on" structures along E-W segments, while it generates *en-échelon* folds and right-lateral shear zones along NW-oriented segments. Interference structures are not shown; just the "freshly formed" structures are schematically indicated.

CONCLUSION AND DISCUSSION ON HYDROCARBON MIGRATION

Summary of Observations on Bitumen Seeps

Several geode- or cavity-types were identified in the field (Figure 22). Some of these were non-conclusive in determining the timing of petroleum migration; others gave useful constraints on timing. Most of the cavities had an identical mineral coating of different generations of calcite, dolomite, and more rarely quartz, precipitated from hydrothermal fluids of different temperature and salinity. This mineral coating was observed irrespective of the age of the host rock.

In deep gorges across Cretaceous–Palaeocene reservoirs some of these bitumen-filled cavities were observed in macrofossils. In most cases, moldic porosity was reduced by mineral coating. These cavities do not provide any age constraint.

Some exposures in Palaeogene marl and dolomitic marl (especially on the Bijell-Dinarta road) revealed cavities filled by angular splinters of wall-rock fragments, that might be assembled to form a more integral original rock volume (Figures 22a and 22b). The cavities were formed by desiccation, dissolution or mineral transformation resulting in volume loss. Later, bitumen filled these cavities. At a quick glance, this type of cavity might be mistaken for a snowball pebble of bitumen, collecting different rock debris as it is rolled by waves across the seashore. This cavity-type and its infill does not give a strong age constraint either, except that this is a diagenetic feature linked to fluid movement, that occurred most probably after deposition.

Some cavities are linked with tectonic surfaces, such as joints (Figure 13), fractures, fault breccias (Figure 20), and shear-related cavities (Figure 6). These cavities have a mineral coating identical to tectonic surfaces without bitumen. Some joints just have a bitumen film, and no coating. These tectonic features, as earlier shown, are linked to several phases of the main NE-SW to N-S shortening of the area, which is dated by the syn-tectonic structures in the Upper Fars and Bakhtiari formations. So these cavity surfaces do provide a timing constraint for migration, i.e. they occurred during or after the Middle Miocene–Pliocene main shortening episode.

Figure 22: Apparent bitumen clasts in Palaeocene rocks. (a) Black, rounded bitumen in whitish Khurmala marl layers; northern limb of Aqra Anticline near Dinarta. (b) Close-up of one of the bitumen balls indicating pieces of rock-wall encased in bitumen. These pieces can be assembled with some space deficit, due to some volume-loss process. It is inferred that "dessication cavities" were formed first, later infilled by bitumen. (c) Apparent bitumen pebbles (arrows) in a coarse polymict conglomerate of Kholosh Formation (Palaeocene) near M'Kerr village, close to Hareer (location in Figure 1b). (d) One of these "bitumen pebbles" indicating a remaining rock crust and the inner space occupied by bitumen. (e) Cut surface of the same pebble indicating that dissolution cracks were formed inside the carbonate pebble, later filled by bitumen.

Even apparently young, non-cemented and brecciated fracture zones are filled with bitumen (Figure 20b). Several large, massive bitumen seeps, and accounts of hillsides burning for several years, suggest that fracturing and hydrocarbon migration to the surface is still ongoing.

The general absence of bitumen in formations younger than the Eocene Gercus Formation speaks for a very effective Gercus seal, and not for migration time preceding Gercus shale.

Cretaceous *versus* Miocene Migration

Earlier interpretations by Dunnington (1958) suggested a Late Cretaceous–Palaeocene migration and massive surface seeps. This interpretation might have been based on the presence of rounded bitumen objects, interpreted as bitumen pebbles, in the Palaeocene Khurmala marl-dolomite and in the Palaeocene Kholosh formations (Figures 22a and 22c).

Near M'Kerr village, in the Mirawa Anticline (Figure 1b), polymict Palaeocene conglomerate (Kholosh Formation) apparently contains bitumen pebbles (Figure 22c). A closer look reveals however, that all these bitumen "pebbles" have a whitish calcite coating on the external surface of the "pebble", growing towards the inner, dissolved part. Bitumen filled the inner space defined by this mineral coating/rock wall (Figure 22d). In other words, the "bitumen pebbles" are in fact cavities, which formed after dissolution of pebbles, and were later filled by overgrown calcite minerals and finally bitumen.

An additional factor suggesting young maturity and migration is formation thickness. There is a widespread agreement amongst earlier and recent petroleum geologists that the main source rock of this region is the Middle Jurassic Sargelu-Naokelekan Formation (e.g. Dunnington, 1958; Pitman et al., 2004). The ca. 1,000 m of overburden provided by just the Cretaceous formations in the study area is insufficient to bring that source rock to maturity with recent heat-flow rate (Ameen, 1992; Pitman et al., 2004; in-house modelling). The uppermost Cretaceous, Palaeocene and Eocene succession can add another 800–1,000 m, but still this thickness is insufficient to initiate maturity due to the low heat flow (Pitman et al., 2004). The thickest sediments were deposited in Late Miocene, Pliocene and Quaternary (Fars and Bakhtiari formations). This late overburden may have been sufficient to initiate hydrocarbon generation from the Sargelu-Naokelekan source rocks (below ca. 3,500m, e.g. Pitman et al., 2004, in-house modeling).

ACKNOWLEDGEMENTS

MOL Plc, Kalegran Ltd and Gulf Keystone Petroleum International are thanked for permission to publish the paper. György Kovács, Kalegran's and József Grill MOL's country manager are thanked for continuous support and encouragement and helpful contributions to fieldwork. The Ministry of Mineral Resources of Kurdistan Regional Government of Iraq and his Eminence Dr Ashti Havrami are thanked for giving us the permission to present the data. The GeoArabia team is acknowledged for technical efforts to take care of the paper. Moujahed Al Husseini, Joerg Mattner and Kathy Breining are especially thanked for proofreading the manuscript. Nestor "Niño" A. Buhay is greatly acknowledged for the high-quality graphics. Great thanks is due to anonymous Reviewer A, who pushed us to present data in a more precise and better understandable way.

REFERENCES

Allen, M.B., J. Jackson, and R. Walker 2004. Late Cenozoic reorganization of the Arabia-Eurasia collision and the comparison of short-term and long-term deformation rates. Tectonics, v. 23.

Ameen, M.S. 1992. Effect of basement tectonics on hydrocarbon generation, migration and accumulation in northern Iraq. American Association of Petroleum Geologists Bulletin, v. 76, p. 356-370.

Blanc, E. J.-P., M.B. Allen, S. Inger and H. Hassani 2003. Structural styles in the Zagros Simple Folded Zone, Iran. Journal of the Geological Society, London, v. 160, p. 401-412.

Bretis, B., N. Bartl and B. Grasemann 2011. Lateral fold growth and linkage in the Zagros fold and thrust belt (Kurdistan, NE Iraq). Basin Research, v. 23, p. 615-630.

Burberry, C.M., J.W. Cosgrowe, and J.-G. Liu 2010. A study of fold characteristics and deformation style using the evolution of the land surface: Zagros Simply Folded Belt, Iran. In P. Letrumy, and C. Robin (Eds.), Tectonic and Stratigraphic Evolution of Zagros and Makran during the Mesozoic–Cenozoic. Geological Society, London, Special Publications, 330, p. 139-154.

Chalabi, A., L. Gagala, J. Vergés, P. Keller, and N. Bang 2010. Structure of Zagros Simply Folded Zone. Abstracts of the 72nd EAGE Conference, Barcelona, 33.

Cochran, J. 1981. The Gulf of Aden: Structure and evolution of a young ocean basin. Journal of Geophysical Research, v. 86, p. 263-287.

Dunnington, H.V. 1958-2005. Generation, migration, accumulation, and dissipation of oil in Northern Iraq. Habitat of Oil (Ed. L.G. Weeks), American Association of Petroleum Geologists, p. 1194-1251. Reprinted by GeoArabia, 2005, v. 10, no. 2, p. 39-84.

Heidbach, O., M. Tingay, A. Barth, J. Reinecker, D. Kurfeß and B. Müller 2008. The World Stress Map database release 2008 doi:10.1594/GFZ.WSM.Rel2008, 2008.

Hessami, K., H. Koyi, C. Talbot, H. Tabasi and E. Shabazian 2001. Progressive unconformities within an evolving foreland fold-thrust belt, Zagros Mountains. Journal of the Geological Society of London, v. 158, p. 969-981.

Homke, S., J. Vergés, M. Garcés, H. Emami and R. Karpuz 2004. Magnetostratigraphy of Miocene–Pliocene Zagros foreland deposits in the front of the Pusht-e Kuh Arc (Lurestan Province, Iran): Earth and Planetary Science Letters, v. 225, p. 397–410, doi: 10.1016/ j.epsl.2004.07.002.

Jassim, S.Z and J.C. Goff 2006. Geology of Iraq. Dolin, Prague and Moravian Museum Publications, Brno. 341p.

Kaymakci, N., Z.M. Inceöz, P. Ertepinar and A. Koc 2010. Late Cretaceous to Recent kinematics of SE Anatolia (Turkey). In M. Sosson, N. Kaymakci, R.A. Stephenson, F. Bergerat and V. Starostenko (Eds.), Sedimentary basin tectonics from the Black Sea and Caucasus to the Arabian Platform. Geological Society of London, Special Publications, 340, p. 409-435.

Lacombe O., F. Mouthereau, S. Kargar and B. Meyer 2006. Late Cenozoic and modern stress fields in the western Fars (Iran): Implications for the tectonic and kinematic evolution of central Zagros. Tectonics, v. 25.

McClay, K.R. and P.S. Whitehouse, 2004. Analogue modelling of doubly vergent thrust wedges, In K.R. McClay, (Ed.), Thrust tectonics and hydrocarbon systems: American Association of Petroleum Geologists Memoir 82, p. 184-206.

Navabpour P., J. Angelier and E. Barrier 2007. Cenozoic post-collisional brittle tectonic history and stress reorientation in the High Zagros Belt (Iran, Fars Province). Tectonophysics, v. 432, p. 101-131.

Navabpour P., J. Angelier and E. Barrier 2008. Stress state reconstruction of oblique collision and evolution of deformation partitioning in W-Zagros (Iran, Kermanshah). Geophysical Journal International, v. 175, p. 755-782.

McQuarrie, N., J.M. Stock, C. Verdel and B.P. Wernicke 2003. Cenozoic evolution of Neotethys and implications for the causes of plate motions, Geophysical Research Letter 30, art. no. 2036, doi:10.1029/2003GL017992.

Pitman J. K., D. Steinshouer and M.D. Lewan 2004. Petroleum generation and migration in the Mesopotamian Basin and Zagros Fold Belt of Iraq: Results from a basin-modeling study. GeoArabia, v. 9, no. 4, p. 41-72.

Peynircioglu, A. A. 2010. Applying paleomagnetic constraints on rotation and deformation of the Arabian Plate since the Eocene in Southeast Turkey. Tectonic Crossroads: Evolving Orogens of Eurasia-Africa-Arabia Conference Abstracts; Palaeomagnetic perspectives on the Africa-Arabia-Eurasia plate interactions Session. Middle East Technical University, Ankara, 60.

Sarbazheri, K.M., I.M. Ghafor and Q.A. Muhammed 2009. Biostratigraphy of the Cretaceous/Tertiary boundary in the Sirwan Valley (Sulaimani Region, Kurdistan, NE Iraq). Geologica Carpathica, v. 60, no. 5, p. 381-396.

Sissakian, V.K. 1997. Geological map of Arbeel and Mahabad Quadrangles. 1: 250.000 State establishment of Geological Survey and Mining, Iraq. Baghdad.

Spaargaren, F. 1987. Geological map of Iraq and southwestern Iran, scale1:1,000,000. Robertson Research Publication.

Talebian, M., and J. Jackson 2002. Offset on the main recent fault of NW Iran and implications for the late Cenozoic tectonics of the Arabia-Eurasia collision zone, Geophysical Journal International, v. 150, p. 422-439.

Talebian, M. and J. Jackson 2004. A reappraisal of earthquake focal mechanisms and active shortening in the Zagros mountains of Iran. Geophysical Journal International, v. 156, p. 506-526.

Twiss, R.J. and E.M. Moores 1992. Structural Geology. Freeman and Co, San Francisco, 532p.

van Bellen, R.C., H.V. Dunnington, R. Wetzel and D.M. Morton 1959-2005. Stratigraphic Lexicon of Iraq. Reprinted by permission of CNRS by Gulf PetroLink, 239 p.

Vernant, P., F. Nilforoushan, D. Hatzfeld, M.R. Abbassi, C. Vigny, F. Masson, H. Nankali, J. Martinod, A. Ashtiani, R. Bayer, F. Tavakoli and J. Chéry 2004. Present-day crustal deformation and plate kinematics in the Middle East constrained by GPS measurements in Iran and northern Oman. Geophysical Journal International, v. 157, p. 381-398.

ABOUT THE AUTHORS

László Csontos *obtained an MSc in Geology in 1983 at the Eötvös University of Sciences, Budapest, Hungary, and defended his PhD in June 1988 at the University of Lille I, France. He spent three months in British Columbia with a mapping team of the Geological Survey of Canada. After his degree he was employed by the Eötvös University, Department of Geology, where he taught structural geology, geological mapping, and general geology. From the early 1990s he was involved in numerous studies for petroleum exploration companies. These studies mostly reported on several aspects of Carpathian geology, but he also participated in overseas works of MOL PLC, Hungary. His expertise covers most of Middle East and Far East, including the Arabian Peninsula, India, Pakistan, Indonesia, and Malaysia. In 2006 he left teaching for a full-time exploration job at MOL. He was charged with field work in the Oman Mountains and in Kurdistan Region of Iraq. He is particularly interested in structural geology, tectonics, and their application in Petroleum Industry.*

lcsontos@mol.hu

Ágoston Sasvári *holds an MSc in structural geology from Eötvös Loránd University of Sciences, Budapest, Hungary, in 2003. After his PhD studies in the same university, he worked as Exploration Geologist at MOL Hungarian Oil and Gas Company focusing on Middle East region. Sasvári is interested in the structural and petroleum geology based on field work, geological mapping and structural analysis in Hawasina Window (Oman), Margala Hills (Pakistan) and Kurdistan Region (Iraq). Additional interests are in structural inversion methods and models. Recently he changed job to Fugro-Robertson*

sasvariagoston@yahoo.com

Tamás Pocsai *obtained an MSc in Geology in 2004 at the Eötvös University of Sciences in Budapest, Hungary. After he graduated he was employed by the Geological Institute of Hungary. In 2006 he left the Institute and joined the MOL Middle East, Africa & Caspian Exploration Department. He was immediately involved to the field work in the Oman Mountains and later to Pakistan and Kurdistan Region of Iraq. His main fields of interest are structural geology and sedimentology.*

tpocsai@mol.hu

László Kósa *obtained MSc in Geology in 1998 at the Eötvös Loránd University of Sciences Budapest, Hungary. He immediately joined MOL Exploration & Production Division, Domestic Exploration Department, which he changed for the Middle East Africa & Caspian Exploration Department in 2005. He participated on several field works in the company, including those in Pakistan and Kurdistan Region of Iraq. His main fields of interest are structural geology and basin analysis.*

lkosa@mol.hu

Azad T. Salae *obtained MSc in Geology in 2001 at the College of Sciences of Baghdad University, Iraq. Since he graduated he has been employed by the Geological Department of Salahaddin University in Kurdistan Region of Iraq. His main fields of interest are field geology and sedimentology.*

azad_thr@yahoo.com

Athar Ali *obtained MSc Geophysics degree in 1994 from Qauide-e-Azam University, Islamabad, Pakistan. He completed his M. Phil in Geology. Since 1994 he has been working with the Pakistani and international exploration and production companies mainly in Pakistan Oilfields Limited, Mari Gas, Petronas, Gulf Petroleum, China National Petroleum Corporation, Ministry of Energy and Mining of Sudan, Kuwait Petroleum and MOL Group at various locations on different projects. He is currently working with MOL Kalegran Ltd. in Kurdistan Region of Iraq as Exploration and Operations Director.*

aathar@mol.hu

Manuscript received September 30, 2010
Revised July 31, 2011
Accepted November 15, 2011